Nuclear PFKP promotes CXCR4-dependent infiltration by T cell acute lymphoblastic leukemia

Xueliang Gao,[1] Shenghui Qin,[2] Yongxia Wu,[3] Chen Chu,[4,5] Baishan Jiang,[4] Roger H. Johnson,[6] Dong Kuang,[2] Jie Zhang,[1] Xi Wang,[2] Anand Mehta,[1] Kenneth D. Tew,[1] Gustavo W. Leone,[6] Xue-Zhong Yu,[3,6] and Haizhen Wang[1,6]

[1]Department of Cell and Molecular Pharmacology & Experimental Therapeutics, Medical University of South Carolina, Charleston, South Carolina, USA. [2]Institute of Pathology, Tongji Hospital, Tongji Medical College, Huazhong University of Science and Technology, Wuhan, Hubei, China. [3]Department of Microbiology and Immunology, Medical University of South Carolina, Charleston, South Carolina, USA. [4]Department of Cancer Biology, Dana-Farber Cancer Institute and [5]Department of Genetics, Blavatnik Institute, Harvard Medical School, Boston, Massachusetts, USA. [6]Hollings Cancer Center, Medical University of South Carolina, Charleston, South Carolina, USA.

PFKP (phosphofructokinase, platelet), the major isoform of PFK1 expressed in T cell acute lymphoblastic leukemia (T-ALL), is predominantly expressed in the cytoplasm to carry out its glycolytic function. Our study showed that PFKP is a nucleocytoplasmic shuttling protein with functional nuclear export and nuclear localization sequences (NLSs). Cyclin D3/CDK6 facilitated PFKP nuclear translocation by dimerization and by exposing the NLS of PFKP to induce the interaction between PFKP and importin 9. Nuclear PFKP stimulated the expression of C-X-C chemokine receptor type 4 (CXCR4), a chemokine receptor regulating leukemia homing/infiltration, to promote T-ALL cell invasion, which depended on the activity of c-Myc. In vivo experiments showed that nuclear PFKP promoted leukemia homing/infiltration into the bone marrow, spleen, and liver, which could be blocked with CXCR4 antagonists. Immunohistochemical staining of tissues from a clinically well-annotated cohort of T cell lymphoma/leukemia patients showed nuclear PFKP localization in invasive cancers, but not in nonmalignant T lymph node or reactive hyperplasia. The presence of nuclear PFKP in these specimens correlated with poor survival in patients with T cell malignancy, suggesting the potential utility of nuclear PFKP as a diagnostic marker.

Introduction

Phosphofructokinase 1 (PFK1) is one of the key regulatory and rate-limiting enzymes in the glycolysis pathway, converting fructose 6-phosphate and ATP to generate fructose 1,6-biphosphate and ADP (1, 2). PFKP (PFK, platelet), one of the 3 isoforms of PFK1, is highly expressed in T cell and B cell leukemias, ascites tumors, breast carcinoma, and glioblastoma. Upregulation of PFKP is associated with progression and poor prognosis in various solid tumors and in leukemia (3–7). Posttranscriptional modifications of PFKP, such as phosphorylation and acetylation, also promote tumor progression (6, 8). Our previous study revealed that PFKP is the major isoform of PFK1 expressed in T cell acute lymphoblastic leukemia (T-ALL) (9). We found that cyclin-dependent kinase 6 (CDK6) phosphorylates PFKP in cancer cells at serine 679, resulting in the dimeric transition of PFKP from its tetrameric form (9). PFKP was recently reported to reside in the nucleus to regulate gene transcription (10), but how PFKP translocates into the nucleus is not clear, and the function of nuclear PFKP in T-ALL has not been defined.

▶ Related Commentary: https://doi.org/10.1172/JCI151295

Authorship note: XG and SQ contributed equally to this work.
Conflict of interest: The authors have declared that no conflict of interest exists.

Submitted: August 10, 2020; **Accepted:** July 1, 2021; **Published:** August 16, 2021.
Reference information: *J Clin Invest*. 2021;131(16):e143119.
https://doi.org/10.1172/JCI143119.

Cyclin and its associated kinases are the core cell proliferation machinery of the cell cycle (11). CDK6 and CDK4 are cyclin D–dependent kinases that function in the first transition from the gap phase (G1) to the cellular DNA synthesis phase (S) to phosphorylate pocket proteins, i.e., RB, RBL1 (p107), and RBL2 (p130), where their functions are considered to be redundant (12–14). CDK4 and CDK6 also phosphorylate other protein substrates to regulate their functions (15). Despite the functional homology between CDK4 and CDK6, increasing evidence suggests that CDK6 has distinct cellular functions from CDK4 in several important aspects (9, 16–18). Our previous studies found that CDK4 and CDK6 have distinct functions in regulating cancer metabolism and immune surveillance. We demonstrated that cyclin D3/CDK6 carry out prosurvival functions in T-ALL via phosphorylating PFKP and pyruvate kinase type M2 (PKM2) (9). We further found that CDK4 destabilizes PD-L1 via cullin 3-SPOP in multiple solid tumors to regulate cancer immune surveillance (18). These studies began to dissect important differences between these two CDK isoforms that may expose distinct vulnerabilities in specific cancer types.

A major indicator of poor prognosis of leukemia is extramedullary infiltration of cancer cells into other organs. It is important to understand the infiltration mechanisms in the interest of developing efficacious therapeutic strategies to prevent or treat extramedullary infiltration in patients with newly diagnosed or relapsed leukemia. CDK6 is highly expressed in T cell malignancies including extranodal NK/T cell lymphoma, nasal type (NK/T), T lymphoblastic lymphoma (T-LBL), and T-ALL (13, 19, 20). Cyclin D3/CDK6 is the major cyclin D/CDK in T-ALL, and the kinase activity

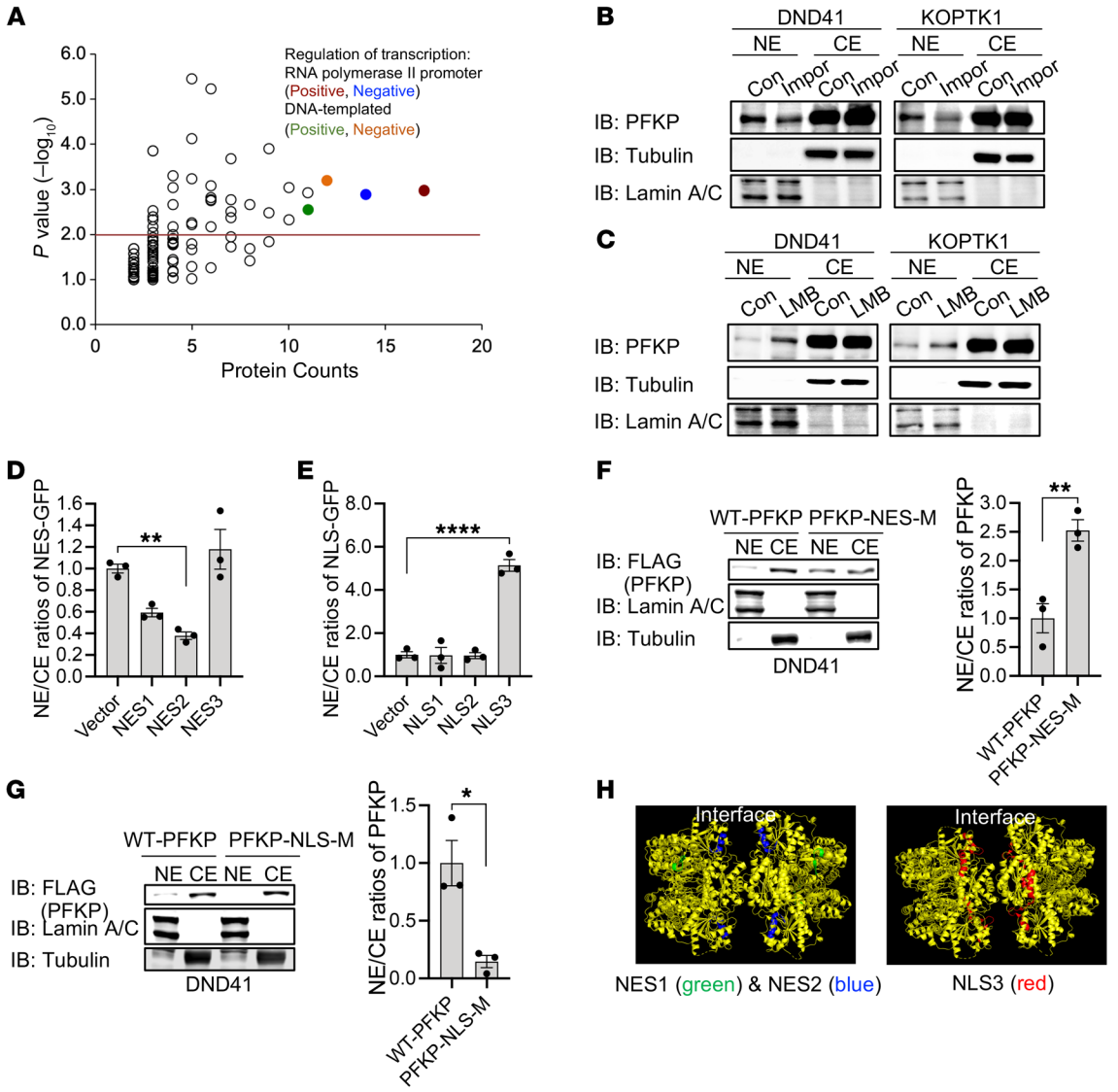

Figure 1. PFKP is a nucleocytoplasmic shuttling protein. (**A**) GO enrichment analysis showing that PFKP interacts with multiple proteins functioning in regulation of nuclear transcription (colored circles with highest protein counts). Source data from 123 literature-curated PFKP-interacting proteins were obtained from the BioGRID database. "Protein Counts" indicates the number of proteins interacting with PFKP in each functional annotation cluster. (**B** and **C**) PFKP nuclear localization relies on importins and exportins. (**B**) Immunoblotting (IB) shows decreased PFKP in nuclear extract (NE) of cells treated with the importin inhibitor, importazole (Impor) (40 μM, 24 hours). (**C**) Increased PFKP in the nuclei of cells treated with the exportin inhibitor, leptomycin B (LMB) (5 ng/mL, 24 hours). CE, cytoplasmic extract. (**D** and **E**) Nuclear-to-cytoplasmic ratios of GFP protein expression from DU145 cells expressing NES-GFP (**D**) or NLS-fused GFP (**E**). IB of GFP was quantified using ImageJ (NIH). GFP vector served as control. (**F**) Nuclear enrichment of PFKP NES mutant. (**G**) Reduced nuclear accumulation of PFKP NLS mutant. In **F** and **G**, IB was performed on the NEs and CEs of cells expressing FLAG-tagged PFKP (left) with an anti-FLAG antibody. The graph on the right shows the NE/CE ratios of FLAG-PFKP. Lamin A/C is a nuclear protein marker. Tubulin is a cytoplasmic protein marker. (**H**) Localization of functional NESs (NES1 in green, NES2 in blue, left) and NLS (in red, right) in the structure of the tetrameric PFKP protein. Functional NLS localizes at the interface in the dimeric form of PFKP. Pymol software was applied for protein structure analysis, and the structure of human PFKP (DOI: 10.2210/pdb4U1R/pdb) was downloaded from the Protein Data Bank (37). $n = 3$ (**B**–**G**). Data represent mean ± SEM. $^*P < 0.05$; $^{**}P < 0.01$; $^{****}P < 0.0001$ by 2-tailed Student's t test (**F** and **G**) or 1-way ANOVA (**D** and **E**).

of CDK6 in T-ALL is enhanced due to its inhibitors, CDKN2A and CDKN2B, being mutated in over 50% of T-ALL cases (21). Targeting CDK6 for T-ALL therapy is promising, as it prevents leukemia cell proliferation and induces apoptosis (9, 13, 20). CDK6 depletion prevents development of lymphoma and T-ALL driven by neurogenic locus notch homolog protein 1 (NOTCH1) (22). CDK6 also appears to play a role in cell migration and metastasis (23–25), but whether and how cyclin D3/CDK6 regulate T-ALL homing/infiltration is not known.

C-X-C chemokine receptor type 4 (CXCR4) is an α-chemokine receptor specific for stromal cell–derived factor 1 (also called CXCL12). CXCR4 is the most commonly reported chemokine receptor in cancer, as it is expressed in at least 23 different types of solid and hematopoietic cancers (26). Besides its critical roles in tumor growth, CXCR4 has also been found to function in mediating cancer cell–tumor microenvironment interaction, angiogenesis, and immunosuppression, which leads to metastasis, drug resistance, and tumor recurrence (27). The expression of CXCR4

Table 1. Predicted NESs/NLSs of PFKP

	Signal sequences
NES1	115-LQRGITNLCV-124
NES2	506-IGGFEAYLGLLEL-518
NES3	624-EKMKTTIQRGLVLRNES-640
NLS1	260-RARKKRLNII-269
NLS2	698-TAKLKEARGRGKKF-711
NLS3	734-ELKKGTDFEHRIPKEQWWLKLRPLMKILAKYK-765

Putative NES/NLS predicted with sequence analysis programs (NES: http://research.nki.nl/fornerodlab/NES-Finder.htm and elm.eu.org; NLS: http://www.moseslab.csb.utoronto.ca/NLStradamus/, NLS-mapper.iab.keio.ac.jp, and elm.eu.org).

in solid tumors can be regulated by several factors, such as hypoxia-inducible factor 1α (HIF-1α) (28), nuclear factor κB (NF-κB), vascular endothelial growth factor (VEGF), basic fibroblast growth factor (bFGF) (29), and epidermal growth factor (EGF) (30). How CXCR4 expression is regulated in hematopoietic cancer has not been thoroughly studied. Further understanding the regulatory mechanisms of CXCR4 expression promises to identify novel therapeutic strategies for cancer patients.

The results presented here indicate that CDK6 promotes T-ALL homing/infiltration by regulating PFKP nuclear localization and CXCR4 expression. Nuclear PFKP may be a useful diagnostic marker for patients with T cell malignancy, as the presence of PFKP in the nucleus is associated with poor overall survival (OS).

Results

PFKP is a nucleocytoplasmic shuttling protein. PFKP, a rate-limiting enzyme in glycolysis, is predominantly located in the cytoplasm (31). A Gene Ontology (GO) enrichment analysis using data from 123 literature-curated PFKP-interacting proteins obtained from the BioGRID database (https://thebiogrid.org/) showed that PFKP interacts with multiple proteins functioning to regulate nuclear transcription (with highest protein counts in the functional annotation clusters) (Figure 1A and Supplemental Tables 1 and 2; supplemental material available online with this article; https://doi.org/10.1172/JCI143119DS1). This suggests that PFKP may translocate into the nucleus to carry out its nuclear function. We confirmed the presence of nuclear PFKP in 2 T-ALL cell lines (DND41 and KOPTK1) by immunoblotting (Figure 1, B and C), but how PFKP translocates into the nucleus is not known. Importin and exportin are the major regulators of nucleocytoplasmic shuttling (32). To investigate whether PFKP is a nucleocytoplasmic shuttling protein and regulated by importin/exportin, we quantified nuclear PFKP levels while blocking the functions of importin or exportin. Treatment with importazole, an importin-β–specific inhibitor, decreased nuclear PFKP levels in leukemia cells (Figure 1B and Supplemental Figure 1A). CRM1 (also known as exportin 1) shuttles a large variety of proteins bearing nuclear export sequences (NESs) to the cytoplasm (33). Leukemia cells treated with leptomycin B (LMB), a CRM1-specific inhibitor, showed increased levels of PFKP in the nucleus (Figure 1C and Supplemental Figure 1B). Importin facilitates nuclear import of proteins by interacting with client nuclear localization sequences (NLSs) (34), whereas exportin regulates nuclear export of protein clients through the recognition of hydrophobic NESs (35). There are 3 potential NLSs and 3 NESs in PFKP according to our amino acid sequence analysis (Table 1). Fusing potential NESs or NLSs individually to green fluorescent protein (GFP) to examine its subcellular localization is an effective method to identify the functions of NESs and NLSs (36). A functional NLS increases the nuclear concentration of NLS-GFP fusion protein; in contrast, a functional NES shifts the distribution of NES-GFP fusion protein toward the cytoplasm. We applied this method to test each potential PFKP NLS or NES in adherent DU145 cells, thereby identifying 2 functional NESs (NES1 and NES2) and 1 functional NLS (NLS3) on PFKP (Figure 1, D and E, and Supplemental Figure 1, C and D). To further validate the nuclear export function of NES1 and NES2, we mutated L122, L513, and L518 to alanine to generate a PFKP-NES mutant tagged by FLAG (PFKP-NES-M). Nuclear amounts of PFKP-NES-M in DND41 and KOPTK1 cells were significantly increased compared with WT-PFKP control (Figure 1F and Supplemental Figure 1E). These results indicate that these functional NESs facilitate nuclear exportation of PFKP. Meanwhile, to examine the function of the identified NLS, we mutated K737, K747, and R755 in NLS3 to alanine (K/R→A) to generate a PFKP-NLS mutant (PFKP-NLS-M). PFKP-NLS-M expression resulted in significantly lower levels of ectopic PFKP accumulation in the nucleus (Figure 1G), suggesting NLS3 is functional in regulating nuclear importation of PFKP. Using the known crystal structure of PFKP (37), we found NES1 localized on the surface, while NES2 was positioned at the dimeric interface of the 3D structure of PFKP (Figure 1H). Of note is that the functional NLS also localized at the dimeric interface of the PFKP model (Figure 1H), which suggests that dimeric, but not tetrameric, PFKP can be imported into the nucleus when the NLS is exposed on the protein surface.

Nuclear translocation of PFKP depends on the kinase activity of CDK6. Our previous study showed that PFKP is present in cells predominantly in its tetrameric and dimeric forms (9). To determine the relative amount of the dimeric form of PFKP in both the nucleus and cytosol, we applied ultrafiltration with a 200-kDa-cutoff membrane to separate dimeric (MW 171 kDa) from tetrameric PFKP (MW 342 kDa), as previously reported (9). The amounts of PFKP in the filtered nuclear extracts (<200 kDa fraction) were then quantified by immunoblotting. Nuclear extract before filtration was loaded as a control. The same method was applied to semiquantify dimeric PFKP in cytoplasmic extract. Higher percentages of dimeric PFKP were found in nuclear compared with cytoplasmic extracts (Figure 2A and Supplemental Figure 2A).

Our previous study showed that cyclin D3/CDK6 phosphorylates PFKP at serine 679 and induces the tetrameric to dimeric transformation of PFKP (9). To test whether cyclin D3/CDK6 facilitates the nuclear translocation of PFKP, we examined nuclear PFKP levels in multiple T-ALL cell lines after treatment with the CDK4/CDK6 inhibitor, palbociclib. CDK4/CDK6 inhibitor treatment dramatically decreased nuclear PFKP abundance, but did not affect total PFKP levels (Figure 2B). To further examine whether cyclin D3 or CDK6 affects nuclear accumulation of PFKP, we genetically knocked down cyclin D3

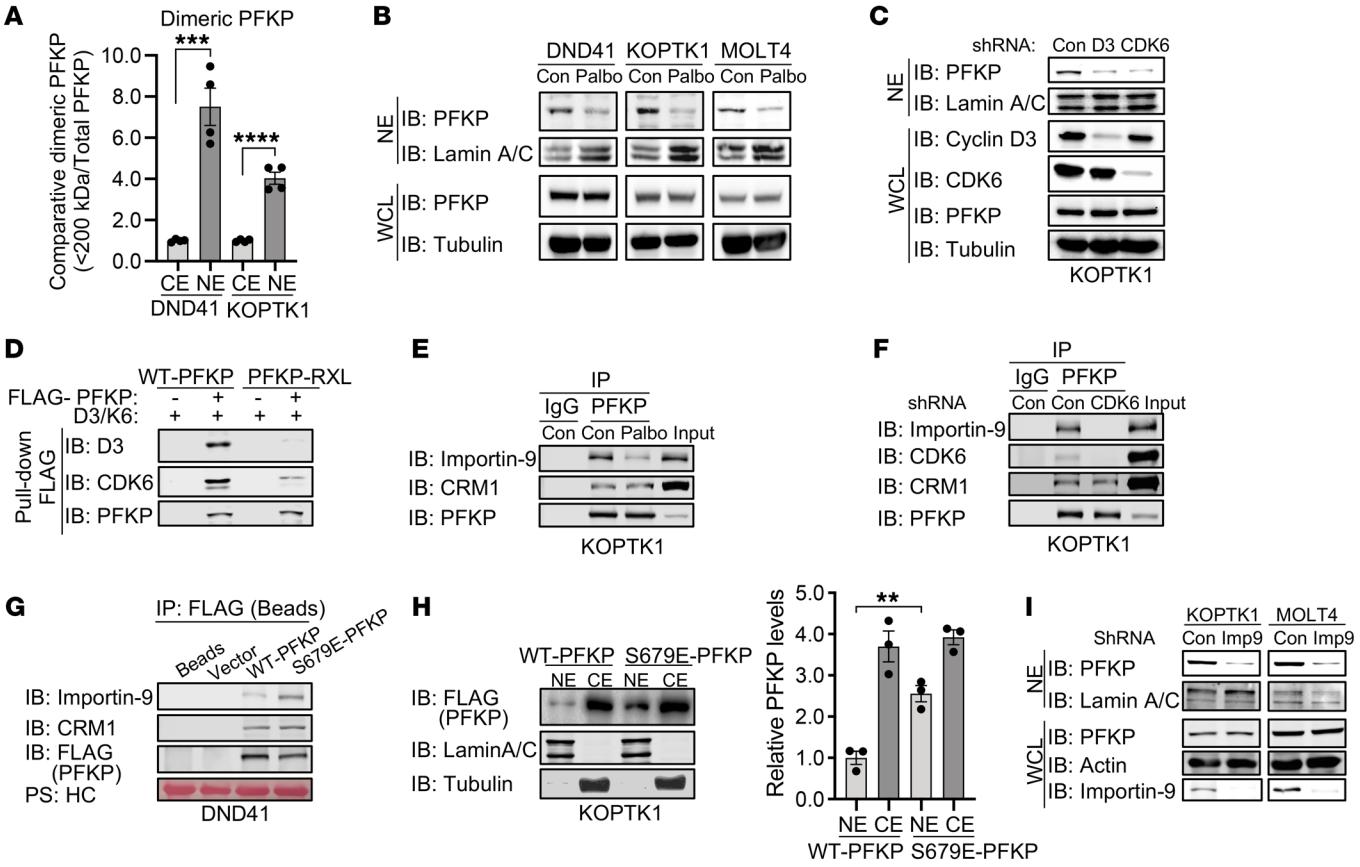

Figure 2. Nuclear localization of PFKP depends on its interaction with cyclin D3/CDK6. (**A**) More dimeric PFKP was detected in the nuclear fraction than in the cytoplasmic fraction. Quantification (ImageJ) was performed by ultrafiltration of nuclear extract (NE) or cytoplasmic extract (CE) from leukemia cells followed by immunoblotting (IB) using an anti-PFKP antibody from Supplemental Figure 2A. (**B**) CDK6 inhibition decreases nuclear accumulation of PFKP. Cells were treated with 1 μM palbociclib (Palbo) or DMSO (Con) for 24 hours. WCL, whole cell lysate. (**C**) Decreased nuclear PFKP in KOPTK1 cells in which either cyclin D3 or CDK6 was knocked down. The knockdown efficiency was examined with IB. (**D**) Pull-down assay using anti-FLAG M2 agarose beads shows direct interaction between FLAG-PFKP and recombinant cyclin D3/CDK6. FLAG peptide served as control. PFKP-RXL is an RXL motif mutant of PFKP. (**E** and **F**) Immunoprecipitation using anti-PFKP antibody–conjugated beads followed by IB showed that the interaction between PFKP and importin-9 was disrupted when CDK6 kinase activity was inhibited (1 μM palbociclib, 24 hours) (**E**) or when CDK6 was knocked down (**F**), while the interaction between PFKP and CRM1 was not affected. (**G**) Immunoprecipitation using anti-FLAG beads followed by IB shows that higher levels of importin 9 co-immunoprecipitated with mutant S679E-PFKP than WT. HC is the heavy chain of the FLAG antibody stained with Ponceau S (PS: HC). (**H**) IB of ectopic PFKP expression in NE or CE of cells expressing S679E- or WT-PFKP (left). FLAG-PFKP expression was normalized to nuclear FLAG from cells expressing WT-PFKP (right). (**I**) IB shows decreased nuclear accumulation of PFKP in importin-9–knockdown cells. IB of WCL shows no significant alteration of PFKP expression. Lamin A/C and actin were used as loading controls. $n = 4$ (**A**) and 3 (**B**–**I**). Data represent mean ± SEM. $^{**}P < 0.01$, $^{***}P < 0.001$, $^{****}P < 0.0001$ by 2-tailed Student's t test (**A**) or 1-way ANOVA (**H**).

or CDK6 using shRNA in KOPTK1 and DND41 cells. Nuclear enrichment of PFKP was significantly reduced in cyclin D3– and CDK6-knockdown leukemia cells, while the total cellular PFKP levels remained constant (Figure 2C and Supplemental Figure 2B). These data indicate that cyclin D3/CDK6 regulates the nuclear enrichment of PFKP.

Cyclin D3/CDK6 interacts with PFKP in multiple T-ALL cell lines (9). To test whether cyclin D3/CDK6 directly interacts with PFKP, we performed in vitro protein-protein pull-down assays. Purified FLAG-tagged PFKP was incubated with recombinant cyclin D/CDK6 protein complex for 30 minutes, and anti-FLAG antibody was applied to pull down proteins associated with PFKP. The results showed that PFKP directly interacted with cyclin D3/CDK6, as cyclin D3/CDK6 was positively detected in the pull-down complex with FLAG-tagged PFKP, but not with control FLAG peptides (Supplemental Figure 2C).

RXL motifs in cyclins are critical for their interaction with partner proteins (38, 39). Amino acid sequence analysis (PDB: 4U1R) revealed 5 potential cyclin-binding RXL motifs in PFKP (Table 2). To test whether these RXL cyclin-binding motifs in PFKP are

Table 2. List of cyclin-binding motifs in the amino acid sequence of PFKP

RXL motif	Sequence
RXL1	319-RIL-321
RXL2	442-RML-444
RXL3	613-RDL-615
RXL4	632-RGL-634
RXL5	755-RPL-757

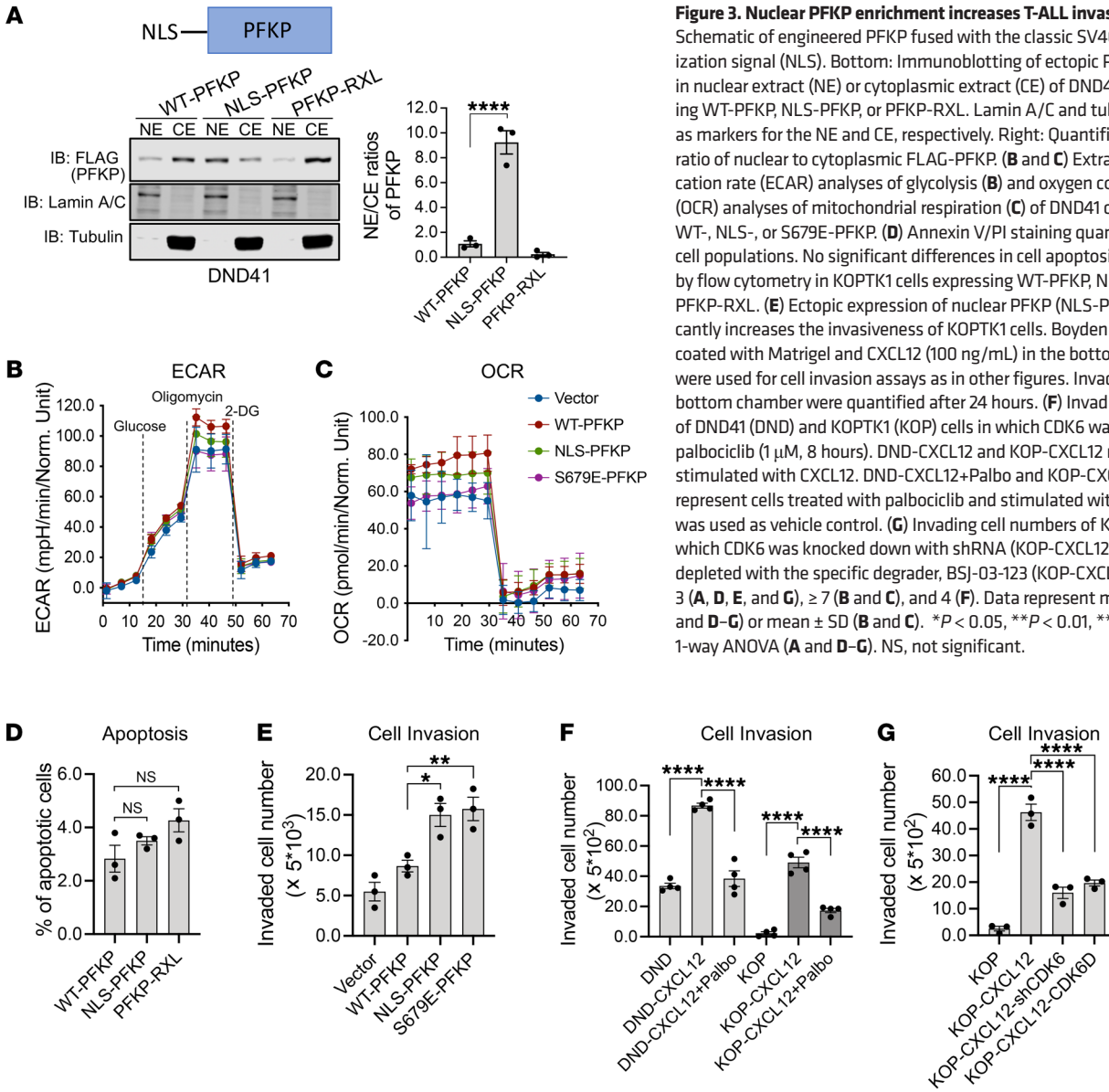

Figure 3. Nuclear PFKP enrichment increases T-ALL invasion. (**A**) Top: Schematic of engineered PFKP fused with the classic SV40 nuclear localization signal (NLS). Bottom: Immunoblotting of ectopic PFKP expression in nuclear extract (NE) or cytoplasmic extract (CE) of DND41 cells expressing WT-PFKP, NLS-PFKP, or PFKP-RXL. Lamin A/C and tubulin were used as markers for the NE and CE, respectively. Right: Quantification of the ratio of nuclear to cytoplasmic FLAG-PFKP. (**B** and **C**) Extracellular acidification rate (ECAR) analyses of glycolysis (**B**) and oxygen consumption rate (OCR) analyses of mitochondrial respiration (**C**) of DND41 cells expressing WT-, NLS-, or S679E-PFKP. (**D**) Annexin V/PI staining quantifies apoptotic cell populations. No significant differences in cell apoptosis were detected by flow cytometry in KOPTK1 cells expressing WT-PFKP, NLS-PFKP, or PFKP-RXL. (**E**) Ectopic expression of nuclear PFKP (NLS-PFKP) significantly increases the invasiveness of KOPTK1 cells. Boyden chambers coated with Matrigel and CXCL12 (100 ng/mL) in the bottom chambers were used for cell invasion assays as in other figures. Invading cells in the bottom chamber were quantified after 24 hours. (**F**) Invading cell numbers of DND41 (DND) and KOPTK1 (KOP) cells in which CDK6 was inhibited by palbociclib (1 μM, 8 hours). DND-CXCL12 and KOP-CXCL12 represent cells stimulated with CXCL12. DND-CXCL12+Palbo and KOP-CXCL12+Palbo represent cells treated with palbociclib and stimulated with CXCL12. DMSO was used as vehicle control. (**G**) Invading cell numbers of KOPTK1 cells in which CDK6 was knocked down with shRNA (KOP-CXCL12-shCDK6) or depleted with the specific degrader, BSJ-03-123 (KOP-CXCL12-CDK6D). n = 3 (**A**, **D**, **E**, and **G**), ≥ 7 (**B** and **C**), and 4 (**F**). Data represent mean ± SEM (**A** and **D**–**G**) or mean ± SD (**B** and **C**). $^{*}P < 0.05$, $^{**}P < 0.01$, $^{****}P < 0.0001$ by 1-way ANOVA (**A** and **D**–**G**). NS, not significant.

required for its interaction with cyclin D3/CDK6, we performed pull-down assays using a PFKP-RXL mutant, in which arginine residues in RXL motifs were replaced with glutamic acids. Purified PFKP-RXL protein from DND41 was utilized to examine the interaction with recombinant cyclin D3/CDK6 protein, as described above. The results showed that the interaction between PFKP-RXL and cyclin D3/CDK6 was disrupted, indicating that the RXL motifs are required for the interaction between PFKP and cyclin D3/CDK6 (Figure 2D). In addition, PFKP-RXL expression was predominantly detected in the cytoplasmic fractions, with almost none being observed in the nuclear fractions. Treatment of KOPTK1 cells with the exportin-specific inhibitor, LMB, did not increase the nuclear amount of PFKP-RXL (Supplemental Figure 2D). This suggests that the decreased nuclear amount of PFKP-RXL is due to inhibition of its nuclear importation, but not to any increase in nuclear exportation. We therefore conclude that the nuclear translocation of PFKP relies on its direct interaction with cyclin D3/CDK6 as well as the kinase activity of CDK6.

CDK6 regulates the interaction between PFKP and importin-9. Importin-9 interacts with CDK6 in both MOLT4 and KOPTK1 leukemia cells, as detected with coimmunoprecipitation (co-IP) followed by mass spectrometry (MS) (refer to published Supplemental Table 1 of ref. 9). Importin-9 is a nuclear transport receptor that regulates nuclear localization of multiple proteins (40). Our preliminary co-IP/MS experiments indicated that importin-9 also interacts with PFKP in both KOPTK1 and JURKAT cells (Supplemental Figure 2E). This raises the possibility that importin-9 might interact with PFKP to regulate its nuclear translocation. We first confirmed the interaction between importin-9 and CDK6, and then importin-9 and PFKP, using co-IP followed by immunoblotting with specific antibodies in both KOPTK1 and MOLT4 cells (Supplemental Figure 2, F and G, and Figure 2E). Remarkably, the interaction between PFKP and importin-9 was disrupted in leukemia cells in which CDK6 kinase activity was inhibited or CDK6 was knocked down with shRNA, indicating that the interaction between PFKP and importin-9 relied on the kinase activity

Table 3. List of cell surface proteins functioning in cell invasion/migration whose transcription was downregulated in KOPTK1 cells treated with CDK6 inhibitor

Protein name	Log_2(Palbo/vehicle)[A]	*P* value	Functions
CXCR4	–1.2	1.30×10^{-5}	Invasion/migration/metastasis
PPFIA4	–1.3	3.06×10^{-5}	–
FGFR3	–1.3	3.59×10^{-5}	Migration/invasion
FZD1	–2	7.37×10^{-5}	–
FZD5	–1.2	5.13×10^{-4}	–
HMMR	–3.3	1.52×10^{-7}	Migration/invasion
VEGFA	–1.3	1.79×10^{-4}	Angiogenesis/metastasis
GPR19	–2.2	1.33×10^{-7}	–
ITPR3	–1.3	5.80×10^{-7}	–
TRPC3	–2.1	1.69×10^{-7}	Migration
VLDLR	–1.6	2.20×10^{-4}	Migration/metastasis
GPSM2	–2.4	8.19×10^{-8}	–

Related to Figure 4A. Original data were obtained from EMBL-EBI (www.ebi.ac.uk), and analyzed with the DAVID 6.8 functional annotation tool (NIH).
[A]Log_2(palbociclib/vehicle) ≤ –1.2-fold.

of CDK6 (Figure 2, E and F, and Supplemental Figure 2, G and H). CRM1-specific inhibitor treatment led to nuclear accumulation of PFKP (Figure 1C). We confirmed the interaction between PFKP and CRM1 using co-IP followed by immunoblotting in lysates of KOPTK1 and MOLT4 cells. Unlike importin-9, the interaction between PFKP and CRM1 did not rely on the kinase activity of CDK6 (Figure 2, E and F, and Supplemental Figure 2, G and H). Taken together, these findings suggest that CDK6 regulates nuclear importation but not exportation of PFKP.

Since more dimeric PFKP localized to the nucleus than to the cytosol (Figure 2A) and nuclear PFKP accumulation depended on CDK6 kinase activity (Figure 2B), we next asked whether a CDK6-dependent phosphomimic of the PFKP mutant (S679E) increased the interaction with importin-9. A pull-down assay followed by immunoblotting showed that indeed, compared with WT-PFKP, a greater amount of importin-9 protein interacted with S679E-PFKP (Figure 2G) and more S679E-PFKP mutant accumulated in the nucleus (Figure 2H). In addition, in both KOPTK1 and MOLT4 cells, nuclear accumulation of PFKP was significantly decreased when importin-9 was knocked down using shRNA, with no obvious change in total cellular levels of PFKP (Figure 2I). IP using an anti-GFP antibody followed by immunoblotting showed that importin-9 interacted with NLS3-GFP fusion protein from DU145 cells, and CRM1 interacted with functional NES1- and NES2-GFP protein (Supplemental Figure 2I). This further suggested that the nucleocytoplasmic shuttling of PFKP depends on its own NLS and NESs, as well as its interaction with karyopherins.

Nuclear PFKP mediated by CDK6 stimulates T-ALL invasion. The nuclear function of PFKP in T-ALL is not known. To understand the role of nuclear PFKP, we engineered an SV40 NLS (MDPKKKRKGR) at the N-terminus of PFKP to increase its nuclear translocation. Immunoblotting showed that NLS-tagged PFKP was enriched in the nucleus relative to WT-PFKP (Figure 3A and Supplemental Figure 3A). PFKP is a key enzyme of glycolysis; thus, we measured glycolysis and mitochondrial respiration of DND41 cells expressing ectopic PFKP using the Seahorse XF instrument. The glycolysis, glycolytic capacity, and glycolytic reserve of cells expressing WT-, NLS-, or S679E-PFKP were not significantly affected compared with cells expressing vector control, which was assessed through extracellular acidification rate (ECAR) measurement (Figure 3B and Supplemental Figure 3B). The oxygen consumption rate (OCR), which reflects mitochondrial respiration, did not significantly change in DND41 cells expressing ectopic PFKP mutants (Figure 3C). Cell cycle analysis using the BrdU/PI staining method showed no significant difference among KOPTK1 cells ectopically expressing NLS-PFKP, WT-PFKP, or PFKP-RXL; and no significant difference in apoptotic index was observed (Supplemental Figure 3C and Figure 3D). Interestingly, expression of NLS-PFKP dramatically promoted invasiveness of KOPTK1 cells (Figure 3E). Since PFKP nuclear translocation depended on the kinase activity of CDK6 (Figure 2B), we then tested whether CDK6 inhibition could affect leukemia cell invasion. Invasiveness was significantly decreased in both DND41 and KOPTK1 cells upon treatment with palbociclib, while total cell number did not change significantly (Figure 3F and Supplemental Figure 3D). Further, CDK6 knockdown with shRNA or depletion with a specific degrader, BSJ-03-123, also dramatically reduced the invasive capability of KOPTK1 cells, indicating that CDK6 performs a key function in leukemia cell invasion (Figure 3G).

Cyclin D3/CDK6–mediated nuclear PFKP translocation regulates CXCR4 expression. Since CDK6 inhibition significantly diminished PFKP nuclear translocation (Figure 2B), we deduced that CDK6 inhibition decreases the nuclear functions of PFKP. To uncover the mechanisms underlying regulation of leukemia cell invasiveness by nuclear PFKP, we analyzed transcription profiling array data of KOPTK1 cells upon treatment with the CDK4/CDK6 inhibitor palbociclib (PD0332991) (EMBL-EBI, www.ebi.ac.uk). A functional annotation tool (DAVID 6.8, NIH; https://david.ncifcrf.gov/) was applied to analyze the enrichments with and without treatment (log_2[palbociclib/vehicle] ≤ –1.2-fold). Annotation clusters with high enrichment score were "cell cycle," "cell division," and "chromosome and DNA damage/repair," all well-known functions of CDK4/CDK6. Notably, 6 of 12 proteins in the annotation cluster "cell surface proteins/receptor functioning in cell invasion/migration/metastasis," including CXCR4, FGFR3, HMMR, and VEGFA, were shown to be downregulated upon treatment with palbociclib (Table 3). We confirmed that the protein levels of CXCR4 and HMMR, but not FGFR3 and VEGFA, were significantly downregulated in multiple leukemia cell lines treated with palbociclib (Figure 4A). CXCR4 expression was significantly reduced in KOPTK1 cells in which CDK6 was either depleted with the CDK6 degrader BSJ-03-123 or knocked down with shRNA (Figure 4B). It is worth noting that regulation of CXCR4 by CDK6 does not depend on the presence of RB proteins, as RB (RB, RBL1, RBL2) knockdown in KOPTK1 and MOLT4 cells did not affect CDK6-mediated CXCR4 expression (Supplemental Figure 4A). This suggests that the regulatory effect of CDK6 on CXCR4 is RB independent. p53 plays a role in cancer metastasis and negatively regulates CXCR4 expression to mediate breast

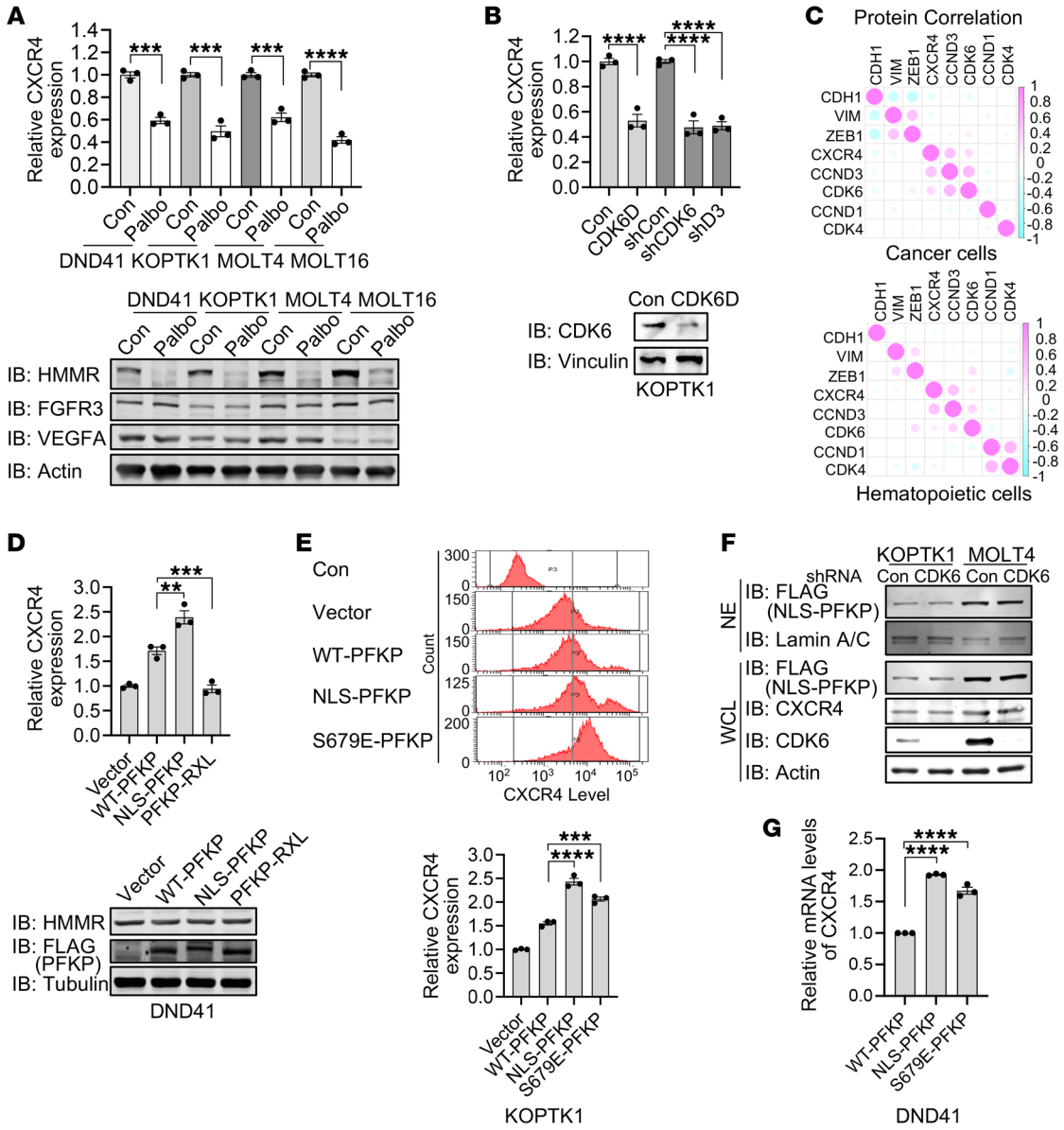

Figure 4. Nuclear PFKP upregulates CXCR4 expression. (**A**) Expression levels of cell surface proteins (upper: CXCR4, by flow cytometry; lower: HMMR, FGFR3 and VEGFA, by immunoblotting [IB]) functioning in cell invasion/migration were measured in leukemia cells treated with palbociclib (Palbo) (1 μM, 48 hours for DND41 and KOPTK1; 1 μM, 24 hours for MOLT4 and MOLT16). (**B**) CXCR4 expression measured by flow cytometry was decreased in KOPTK1 cells treated with the CDK6 degrader (CDK6D; 10 μM BSJ-03-123, 48 hours), or in which CDK6/cyclin D3 was knocked down with shRNA. IB shows the efficiency of the CDK6 degrader. Actin and vinculin were loading controls. (**C**) Correlation analysis of CCLE transcriptomic data reveals that expression of *CCND3* (encoding cyclin D3) and *CDK6*, but not of *CCND1* (encoding cyclin D1) or *CDK4*, is correlated with that of *CXCR4* in all cancer cell lines (1,019 cell lines in total) and in hematopoietic cell lines (176 cell lines in total). Purple color represents positive correlation, and blue color represents negative correlation. Larger size and darker color of the dots represent stronger correlation between two genes. Pearson's correlation coefficients for each pair of genes were calculated using R software. (**D**) CXCR4 expression measured by flow cytometry was increased in cells expressing NLS-PFKP but not PFKP-RXL (upper). IB shows HMMR expression was not changed in cells expressing NLS-PFKP or PFKP-RXL mutant (lower). (**E**) Flow cytometry analysis of CXCR4 expressed on the surface of KOPTK1 cells (upper), in which the median value of the reading was used for quantification (lower). CXCR4 expression was normalized to KOPTK1 cells transfected with empty vector. (**F**) CDK6 knockdown in leukemia cells expressing NLS-PFKP did not significantly affect nuclear PFKP accumulation (upper). IB of whole cell lysate (WCL) showed that the expression of NLS-PFKP or CXCR4 was not affected by CDK6 knockdown (lower). (**G**) Fold changes in mRNA levels of *CXCR4* in cells expressing NLS-PFKP compared with WT-PFKP measured using qRT-PCR. $n = 3$ (**A**, **B**, and **D**–**G**). Data represent mean ± SEM. $^{**}P < 0.01$, $^{***}P < 0.001$, $^{****}P < 0.0001$ by 2-tailed Student's t test (**A**) or 1-way ANOVA (**B**, **D**, **E**, and **G**).

cancer cell invasion (41, 42). To test whether p53 is involved in the downregulation of CXCR4 by CDK6 inhibition, we measured CXCR4 expression in leukemia cell lines (KOPTK1 and MOLT4) in which p53 was knocked down and CDK6 was inhibited by treatment with palbociclib. We found that p53 knockdown had no effect on the downregulation of CXCR4 expression mediated by CDK6 inhibition (Supplemental Figure 4B and Figure 4A). This suggests that p53 is not involved in this regulatory process.

Furthermore, bioinformatic analyses showed that the expression levels of *CCND3* (encoding cyclin D3) correlated well with those of *CXCR4* in 1,019 cancer cell lines based on the Cancer Cell Line Encyclopedia (CCLE) data (https://portals.broadinstitute.org/ccle) (Figure 4C). In all 1,019 cancer cell lines, *ZEB1* (zinc finger E-box binding homeobox 1) expression showed a positive correlation with *VIM* (vimentin), and these two both negatively correlated with *CDH1* (E-cadherin), observations consistent with prior knowledge that were applied as controls for the analysis. Importantly, *CCND3* expression positively correlated with that of *CXCR4*, to almost the same extent as the correlation between *ZEB1* and *VIM* (Pearson's *r* of approximately 0.45), which can be considered a strong correlation. In 176 hematopoietic cell lines, the correlations between EMT markers are absent, but the correlation between *CCND3* and *CXCR4* still stands (Figure 4C).

We then examined whether nuclear PFKP increased CXCR4 expression. The expression of CXCR4, but not HMMR, in leukemia cells expressing NLS-PFKP was significantly increased compared with cells expressing WT-PFKP (Figure 4, D and E, and Supplemental Figure 4, C and D). In contrast, expression of the PFKP-RXL mutant showing no nuclear accumulation of PFKP did not increase CXCR4 expression. Leukemia cells expressing S679E-PFKP, which had enriched nuclear distribution of PFKP, showed elevated CXCR4 expression levels compared with WT-PFKP (Supplemental Figure 4D). Knockdown of PFKP in DND41 cells significantly reduced CXCR4 expression, further confirming PFKP's role in regulating CXCR4 expression (Supplemental Figure 4E). All these results suggest that nuclear translocation of PFKP mediated by CDK6 promotes CXCR4 expression to increase cell invasiveness. Notably, CDK6 depletion in leukemia cells expressing NLS-PFKP affected neither the nuclear accumulation of NLS-PFKP nor expression of CXCR4 (Figure 4F), indicating that CDK6 does not have a scaffolding function for nuclear PFKP. Real-time PCR results showed that CXCR4 mRNA levels significantly increased in DND41 and MOLT4 cells expressing NLS-PFKP (Figure 4G and Supplemental Figure 4F), which suggests that upregulation of CXCR4 by nuclear PFKP is likely at the transcriptional level. BioGRID database analysis showed that PFKP interacts with multiple transcription factors (e.g., Myc, SOX2, ZBTB38) as well as chromatin modifiers (e.g., HDAC2, HDAC6, KAT5) (Supplemental Figure 4G), indicating that nuclear PFKP might regulate CXCR4 transcription by interacting with and/or regulating the activities of certain transcription factor(s).

Nuclear PFKP interacts with c-Myc to regulate CXCR4 expression. Analysis of the PFKP-interacting transcription factors listed in Supplemental Figure 4G revealed that c-Myc binds at the promoter region of CXCR4 in multiple cell lines with highest potential cutoff (Supplemental Figure 5A; data retrieved from http://cistrome.org/db/#/), raising the possibility that nuclear PFKP interacts with c-Myc to regulate CXCR4 transcription. c-Myc is a multifunctional transcription factor regulating cellular growth, metabolism, and cell invasiveness (43, 44). Using co-IP followed by immunoblotting, we confirmed that PFKP interacted with c-Myc in DND41 cells, and that their interaction increased when nuclear PFKP was enriched (NLS- and S679E-PFKP) (Figure 5A). c-Myc phosphorylation at serine 62, which stabilizes c-Myc and increases its activity, was increased in cells expressing NLS- or S679E-PFKP. No change in c-Myc phosphorylation at threonine 58, which induces c-Myc degradation, was observed (Figure 5A).

Analysis of ChIP-seq data from 2 cell lines (H2171 and HCT116) revealed several potential c-Myc–binding regions at the CXCR4 promoter (Supplemental Figure 5B). ChIP followed by quantitative PCR (ChIP-qPCR) assay using anti–c-Myc or anti-PFKP antibodies showed that both c-Myc and PFKP bind to the same promoter region of CXCR4 (peak number 31237 from H2171, peak number 42093 from HCT116) (Supplemental Figure 5B), but nuclear PFKP was no longer able to bind to the CXCR4 promoter region when c-Myc was knocked down with shRNA (Figure 5B). Furthermore, CXCR4 expression levels were no longer increased in c-Myc–knockdown cells (Figure 5C), and consequently no increase in nuclear PFKP–mediated cell invasion was observed (Figure 5D and Supplemental Figure 5C). All these results suggested that nuclear PFKP requires c-Myc to upregulate CXCR4 expression and cell invasiveness. To test whether c-Myc activity is critical for PFKP-regulated CXCR4 transcription, we stably introduced CXCR4 promoter–dual luciferase reporter gene fusions into DND41 cells expressing WT-, NLS-, or S679E-PFKP. CXCR4 promoter activity was significantly increased in cells expressing nuclear PFKP (Figure 5E). Moreover, CXCR4 promoter activity was dramatically decreased when c-Myc activity was inhibited by JQ1, the BET bromodomain BRD4 inhibitor (45) (Figure 5E). Cell invasiveness was significantly inhibited by either JQ1 (Supplemental Figure 5D) or a specific inhibitor of c-Myc, 10058-F4 (46–48) (Figure 5F and Supplemental Figure 5E). These findings demonstrate that c-Myc is required for nuclear PFKP control of CXCR4 transcription.

Cell invasiveness promoted by nuclear PFKP relies on CXCR4. Overexpression of CXCR4 is associated with leukemia homing and infiltration (49). Chemokine CXCL12, the ligand for CXCR4, stimulates invasiveness of CXCR4-expressing cells (50, 51). To determine the significance of CXCR4 in cell invasion regulated by nuclear PFKP, we applied CXCR4-specific antagonists (plerixafor or motixafortide), which interfere with the chemotactic interaction between CXCR4 and CXCL12 (52, 53), to block invasion of KOPTK1 and DND41 cells expressing NLS-PFKP. Human CXCL12 was added to cell culture medium in the bottom chambers of invasion assays to stimulate cell invasion. Leukemia cells expressing NLS-PFKP or S679E-PFKP, but not PFKP-RXL, exhibited enhanced invasive capabilities compared with cells expressing WT-PFKP. The enhanced invasiveness was inhibited by CXCR4 antagonists or CXCR4 depletion with shRNA (Figure 6, A and B, and Supplemental Figure 6A). We excluded the possibility that the decreased cell invasion was due to an alteration in total cell number (Supplemental Figure 6A and Supplemental Figure 6, B and C). These results suggest that CXCR4 is the major factor regulated by NLS-PFKP to promote leukemia cell invasiveness.

To further test whether nuclear PFKP stimulates leukemia cell homing/infiltration, we performed an in vivo study using previously established leukemia mouse models (9). KOPTK1 cells expressing NLS-PFKP, WT-PFKP, or PFKP-RXL were i.v. delivered into immunodeficient mice. The mice were then treated with the CXCR4 antagonist, plerixafor, daily for 3 weeks to determine whether it can inhibit nuclear PFKP–induced leukemia cell dissemination. Dissemination of KOPTK1 cells in multiple mouse organs was detected with flow cytometry by

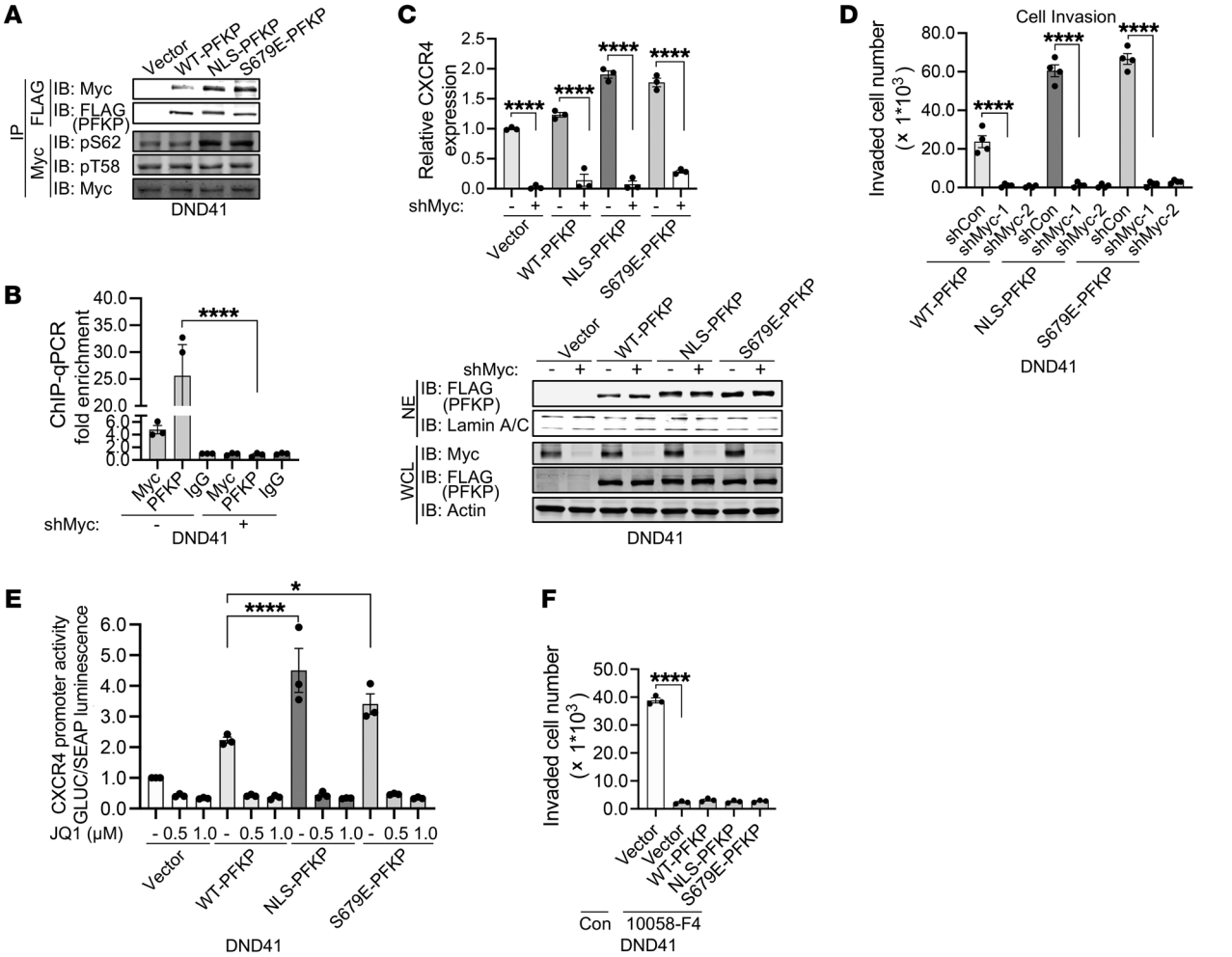

Figure 5. Nuclear PFKP interacts with c-Myc to regulate CXCR4 transcription. (**A**) Immunoblots show that PFKP interacts with c-Myc (upper). Exogenous PFKP was immunoprecipitated from lysates of DND41 cells expressing WT-, NLS-, or S679E-PFKP using an anti-FLAG antibody. The presence of c-Myc was determined by immunoblotting (IB). Phosphorylation of c-Myc at S62, but not T58, increases in cells expressing nuclear PFKP (NLS- or S679E-PFKP) (lower). c-Myc was immunoprecipitated from lysates of DND41 cells expressing WT-, NLS-, or S679E-PFKP. Phosphorylation of c-Myc was determined by IB. c-Myc IB shows the loading of c-Myc proteins. (**B**) ChIP-qPCR shows c-Myc and PFKP binding to the same promoter region of CXCR4. c-Myc and PFKP antibodies were applied to ChIP in formaldehyde-fixed DND41 cells, in which c-Myc was either intact or knocked down with shRNA. Mouse IgG served as a control. (**C**) c-Myc knockdown decreases CXCR4 expression as measured by flow cytometry (upper) but does not affect PFKP expression and its nuclear distribution (lower). c-Myc expression was knocked down in DND41 cells expressing WT-, NLS-, or S679E-PFKP. Expression of nuclear PFKP and c-Myc were examined by IB (lower). (**D**) c-Myc knockdown with independent shRNAs (shMyc-1 or shMyc-2) significantly decreases the invasive capability of DND41 cells expressing WT-, NLS-, or S679E-PFKP. shCon is nontargeting control shRNA. (**E**) Luciferase reporter assay shows c-Myc inhibition decreases CXCR4 promoter activity. DND41 cells expressing WT-, NLS-, S679E-PFKP, or empty vector were treated with JQ1 (0.5 or 1.0 μM) for 48 hours. (**F**) c-Myc inhibitor (50 μM 10058-F4) treatment decreases the invasiveness of DND41 cells expressing WT-, NLS-, or S679E-PFKP. Con is a vehicle control. $n = 3$ (**A**–**C**, **E**, and **F**) and 4 (**D**). Data represent mean ± SEM. $^*P < 0.05$, $^{***}P < 0.001$, $^{****}P < 0.0001$ by 2-tailed Student's t test (**C**) or 1-way ANOVA (**B** and **D**–**F**).

gating on human CD45, a human T cell marker. Similar numbers of KOPTK1 cells expressing NLS-PFKP, WT-PFKP, and PFKP-RXL were detected in peripheral blood. Compared with those expressing WT-PFKP or PFKP-RXL, more KOPTK1 cells expressing NLS-PFKP were detected in bone marrow, spleen, and liver, indicating that leukemia cells expressing nuclear PFKP have higher homing/infiltration rates than those expressing primarily cytosolic WT-PFKP or PFKP-RXL. Plerixafor treatment significantly inhibited homing/infiltration of leukemia cells expressing NLS-PFKP to bone marrow, spleen, and liver, but not the number of leukemia cells in the peripheral blood (Figure 6C). This supports the idea that CXCR4 is the dominant regulator of extramedullary infiltration by leukemia cells expressing NLS-PFKP into multiple organs. The presence of leukemia cells detected by immunohistochemistry (IHC) with an anti–human CD45 antibody showed that leukemia cells indeed homed/infiltrated into the bone marrow, spleen, and liver and supported the notion that accumulation of leukemia cells in these organs is not due to an increase in the number of leukemia cells in the blood vessels (Figure 6D and Supplemental Figure 6D), and that the increased number of malignant cells in these organs is not due to increased proliferation (Supplemental Figure 6E).

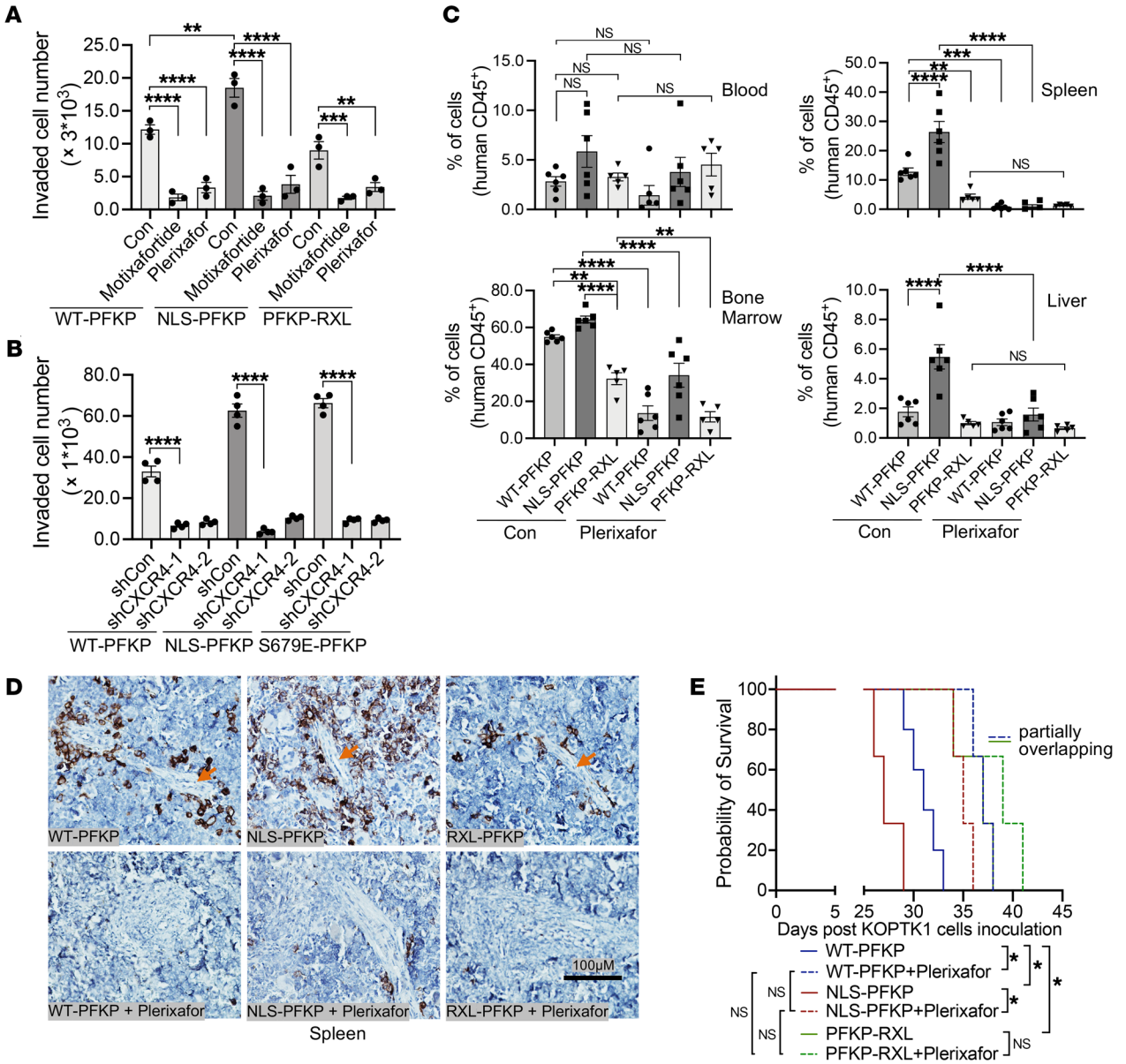

Figure 6. CXCR4 inhibition decreases leukemia cell invasiveness both in vitro and in vivo. (**A**) CXCR4-specific-antagonist treatment of KOPTK1 cells expressing WT-PFKP, NLS-PFKP, or PFKP-RXL significantly decreases cell invasiveness in vitro. Invasion assays were performed on cells with and without treatment with either motixafortide (4 μM) or plerixafor (10 μM). Boyden chambers coated with Matrigel and CXCL12 (100 ng/mL) in the bottom chambers were used for cell invasion assay as in other figures. (**B**) CXCR4 knockdown with shCXCR4-1 or shCXCR4-2 significantly decreases the invasive capability of DND41 cells expressing WT-, NLS-, or S679E-PFKP. shCon is nontargeting control shRNA. (**C**) Flow cytometry analysis of KOPTK1 cells expressing WT-, NLS-PFKP, or PFKP-RXL in peripheral blood, bone marrow, spleen, or liver of immunodeficient mice by gating on human CD45 3 weeks after the mice were tail vein injected with KOPTK1 cells and treated with CXCR4 antagonist (plerixafor) daily. Tissues were dissociated by collagenase treatment followed by passing through a 70-μm strainer. Percentage of cells represents KOPTK1 cells over total gated cells. Each symbol represents data for an individual mouse. (**D**) Immunohistochemical staining with an anti–human CD45 antibody of spleens from mice that received KOPTK1 cells expressing WT-, NLS-PFKP, or PFKP-RXL. Tumor-bearing mice were treated with plerixafor (lower) or vehicle control (upper). Arrows indicate blood vessels. Scale bar: 100 μm. (**E**) Kaplan-Meier survival curves of tumor-bearing mice that received KOPTK1 cells expressing WT-, NLS-PFKP, or PFKP-RXL. Tumor-bearing mice were treated with CXCR4 antagonist (plerixafor) daily, 7 days after the implantation of KOPTK1 cells. $n = 3$ (**A**), 4 (**B**), and 6 (**C** and **D**) mice/group for WT-PFKP and NLS-PFKP, $n = 5$ mice/group for PFKP-RXL; $n = 5$ mice/group (**E**). Data represent mean ± SEM. $^*P < 0.05$, $^{**}P < 0.01$, $^{***}P < 0.001$, $^{****}P < 0.0001$ by 1-way ANOVA (**A**–**C**). NS, not significant.

We next tested how nuclear PFKP affects the survival of tumor-bearing mice. KOPTK1 cells expressing NLS-PFKP, WT-PFKP, or PFKP-RXL were i.v. delivered into immunodeficient NOG mice. Tumor-bearing mice with NLS-PFKP had the poorest survival, while the PFKP-RXL mice had the best. Treatment with plerixafor daily starting 1 week after tumor cell implantation significantly prolonged survival of tumor-bearing mice (Figure 6E). This result suggests that high nuclear PFKP expression leads to rapid leukemia progression and poor survival. The prolongation of survival by CXCR4 antagonist

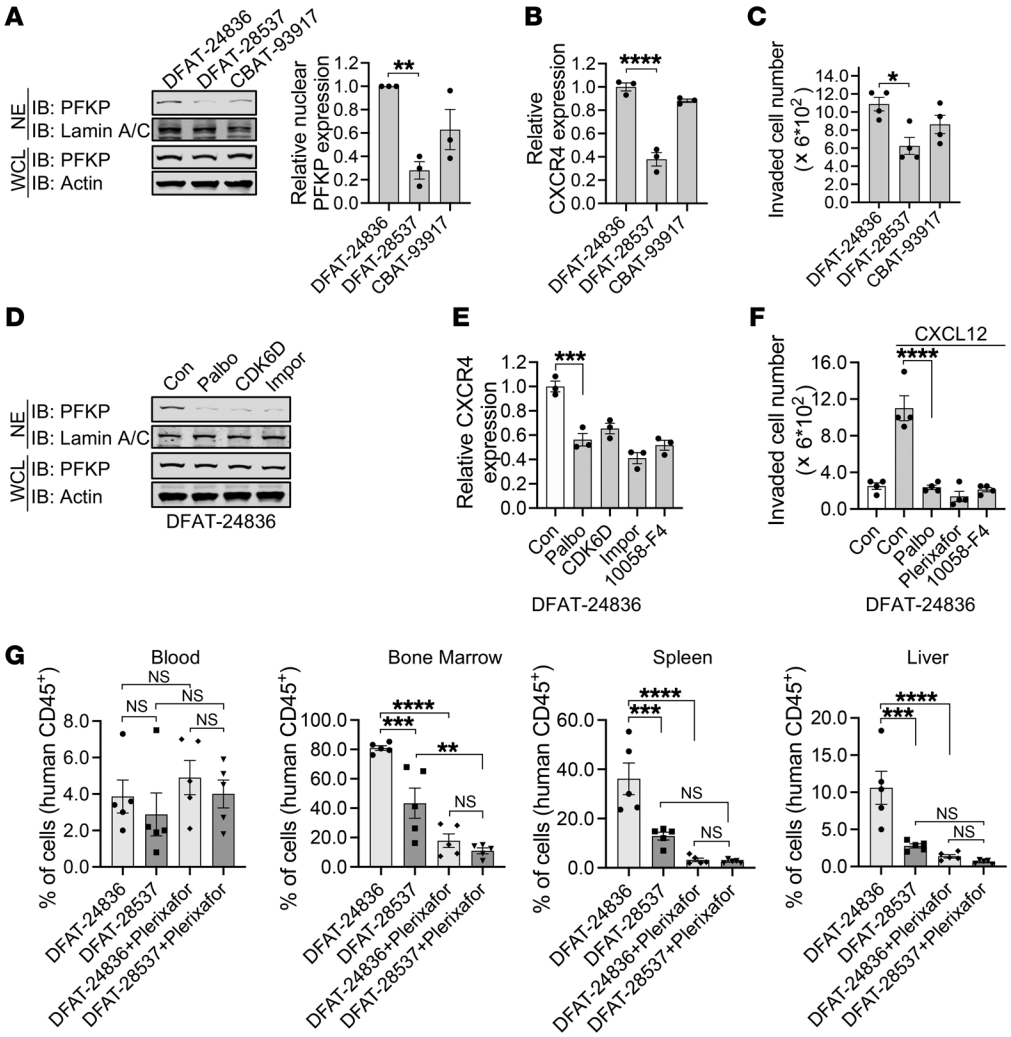

Figure 7. CXCR4 inhibition decreases primary T-ALL invasion. (**A**) Immunoblotting (left) with quantification (right) shows nuclear PFKP expression in primary T-ALL cells from different patients. The 3 primary cultures are designated DFAT-24836, DFAT-28537, and CBAT-93917. (**B**) CXCR4 expression levels in primary T-ALL cells from different patients were analyzed with flow cytometry. (**C**) Invasive capability of primary T-ALL cells from different patients was analyzed. Boyden chambers coated with Matrigel and CXCL12 (100 ng/mL) in the bottom chambers as a stimulus for 24 hours were used for in vitro invasion assays here and Supplemental Figure 7. (**D**) Nuclear PFKP expression in primary T-ALL cells (DFAT-24836) treated with the CDK4/6 inhibitor palbociclib (Palbo, 1 μM), CDK6 degrader (CDK6D; BSJ-03-123, 10 μM), or importin inhibitor importazole (Impor, 40 μM) for 24 hours. (**E**) CXCR4 expression analyzed with flow cytometry in primary T-ALL cells (DFAT-24836) treated with palbociclib (Palbo, 1 μM), BSJ-03-123 (CDK6D, 10 μM), importazole (Impor, 40 μM), or c-Myc inhibitor (10058-F4, 50 μM) for 24 hours. (**F**) Invasion assay of primary T-ALL cells (DFAT-24836) treated with palbociclib (Palbo, 1 μM), CXCR4 antagonist (plerixafor, 10 μM), or c-Myc inhibitor (10058-F4, 50 μM) for 24 hours. (**G**) Analysis of primary T-ALL cells (DFAT-24836 and DFAT-28537) in peripheral blood, bone marrow, spleen, or liver of NOG mice using flow cytometry with gating on human CD45 after the mice were tail vein injected with primary T-ALL cells and then treated with plerixafor daily for 29 days. Percentage of cells represents primary T-ALL over total gated cells. Each symbol represents data for an individual mouse. n = 5 mice/group. n = 3 (**A**, **B**, **D**, and **E**) and 4 (**C** and **F**). Data represent mean ± SEM. $^{*}P < 0.05$, $^{**}P < 0.01$, $^{***}P < 0.001$, $^{****}P < 0.0001$ by 1-way ANOVA (**A**–**C** and **E**–**G**). NS, not significant.

treatment indicates that progression of leukemia expressing nuclear PFKP depends significantly on CXCR4.

Glycolysis inhibition prevents PFKP nuclear translocation and CXCR4 expression. The extracellular signal(s) that stimulate nuclear translocation of PFKP have not been identified. Increased glycolysis correlates with cancer cell invasion and metastasis (54). A previous study showed that the transcriptional regulatory function of PFKP is downregulated when glycolysis is inhibited (10). In addition, inhibition of glycolysis using 2-deoxyglucose (2-DG) induces the expression of p21, which leads to inactivation of cyclin D/CDK. Together, these observations raise the possibility that nuclear translocation of PFKP might be regulated by glycolysis. To test this, we treated T-ALL cells with the glycolytic inhibitor 2-DG, and then quantified nuclear enrichment of PFKP. Nuclear PFKP was significantly reduced upon inhibition of glycolysis, while total cellular PFKP remained unchanged (Supplemental Figure 6F and data not shown). In addition, we found that inhibition of glycolysis downregulated CXCR4 expression (Supplemental Figure 6G). These findings suggest that glycolysis regulates the nuclear translocation of PFKP as well as CXCR4 expression, and that downregulation of glycolysis may prevent nuclear translocation of PFKP and decrease leukemia cell infiltration.

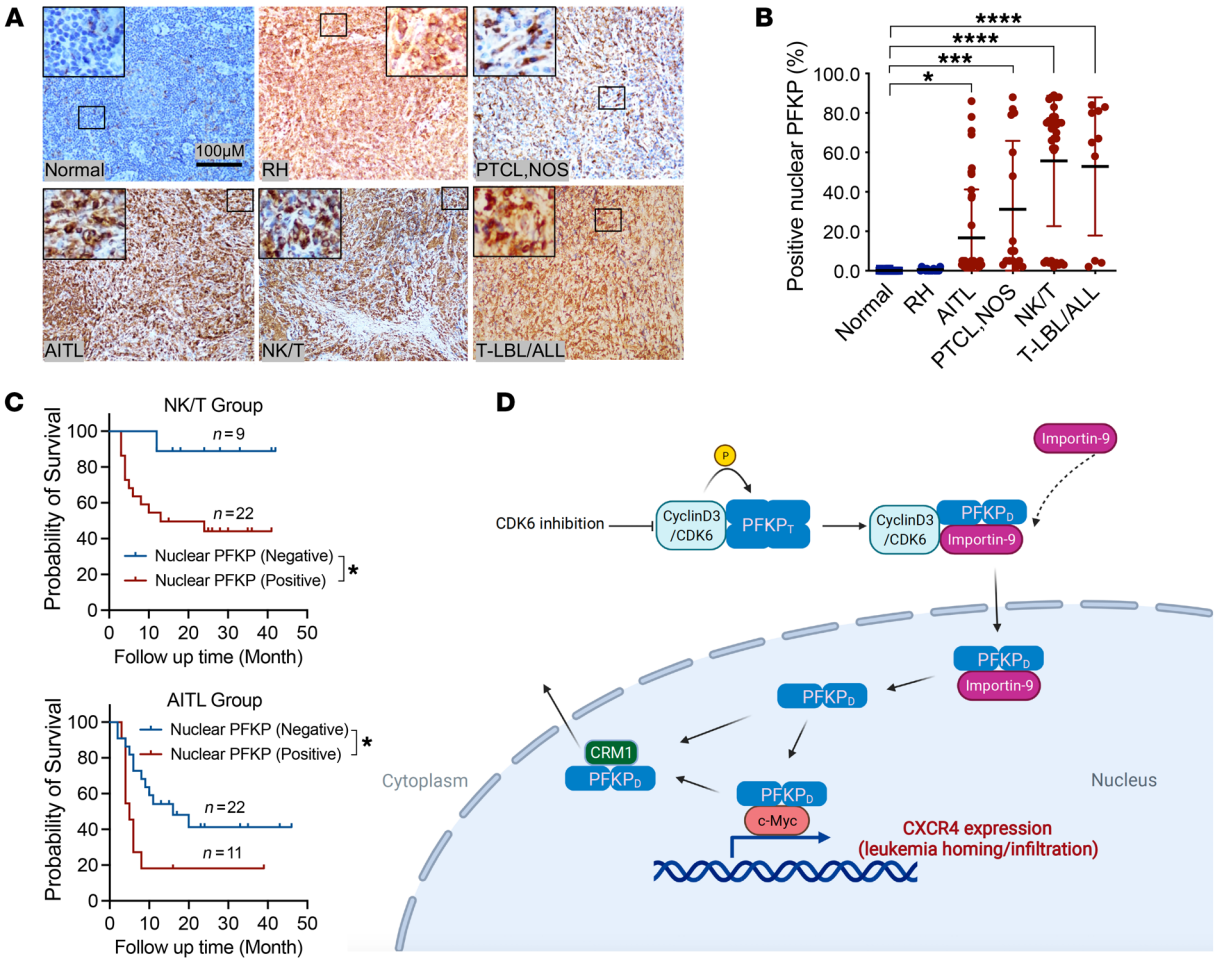

Figure 8. Nuclear PFKP is associated with the aggressiveness of T cell lymphoma/leukemia. (**A**) Immunohistochemistry (IHC) shows nuclear localization of PFKP in aggressive T cell lymphoma/leukemia. High-magnification image represents area indicated by the small rectangle. RH, reactive hyperplasia; PTCL, NOS, peripheral T cell lymphoma, not otherwise specified; AITL, angioimmunoblastic T cell lymphoma; NK/T, extranodal NK/T cell lymphoma, nasal type; T-LBL/ALL, T lymphoblastic lymphoma/acute lymphoblastic leukemia. Scale bar: 100 μm. (**B**) Percentage of positive nuclear PFKP staining in individual specimens. In total, 36 cases of normal, 16 cases of RH, 42 cases of AITL, 16 cases of PTCL, NOS, 33 cases of NK/T, and 10 cases of T-LBL/ALL were analyzed. (**C**) Positive nuclear PFKP staining is associated with poor survival in NK/T and AITL patients. Kaplan-Meier plot of overall survival of patients with negative or positive nuclear PFKP staining in NK/T and AITL groups. Red and blue lines represent patients positive and negative for nuclear PFKP staining, respectively. (**D**) Schematic showing that PFKP is a nucleocytoplasmic shuttling protein with functional nuclear export signal (NES) and nuclear localization signal (NLS) sequences. Cyclin D3/CDK6 facilitates PFKP nuclear translocation by exposing the NLS of PFKP, promoting the interaction between PFKP and importin-9. Nuclear PFKP stimulates the expression of CXCR4 to promote T-ALL cell invasiveness, which depends on the transcription factor c-Myc. Created with BioRender.com. *$P < 0.05$, ***$P < 0.001$, ****$P < 0.0001$ by 1-way ANOVA (**B**).

Invasion by primary T-ALL cells depends on nuclear PFKP translocation and CXCR4 activity. We tested the clinical significance of nuclear PFKP and CXCR4 in the homing/infiltration of tumor cells in 3 primary T-ALL cell cultures from different patients (55). We found that primary T-ALL cells exhibiting high levels of nuclear PFKP showed enhanced CXCR4 expression and invasive capability (Figure 7, A–C). Consistent with the observations in T-ALL cell lines, PFKP nuclear enrichment and CXCR4 expression in primary T-ALL cells depended on the activities of CDK6 kinase and importin; and inactivation of CDK6, c-Myc, or CXCR4 significantly decreased leukemia cell invasiveness (Figure 7, D–F, and Supplemental Figure 7, A–E). An in vivo study using immunodeficient mice further confirmed that primary T-ALL cells with high nuclear PFKP expression showed enhanced homing/infiltration capability, which depended on CXCR4 (Figure 7G).

Our previous study showed that cyclin D3/CDK6 phosphorylates PFKP in melanoma cells with high expression levels of cyclin D3/CDK6 (9). To test whether CDK6 also regulates CXCR4 expression in melanoma, we examined the expression of CXCR4 in 4 melanoma cell lines with various expression levels of cyclin D3/CDK6 (Supplemental Figure 7F). CDK4/CDK6 inhibitor treatment did not significantly affect CXCR4 expression in these cells (Supplemental Figure 7G), which suggests that the regulatory mechanism of CXCR4 expression in melanoma is different from T-ALL.

Nuclear PFKP is enriched in aggressive T cell lymphoma/leukemia tissue specimens, and correlates with low survival rates. Our immunoblotting results demonstrated the presence of PFKP in the nuclear lysates of T-ALL cells (Figures 1B and 7A). To investigate the clinical relevance of nuclear PFKP in T cell malignancy, we performed IHC to analyze PFKP nuclear accumulation

Table 4. Correlation between PFKP nuclear expression levels and clinicopathological features in patients with AITL

Patient characteristics		Nuclear PFKP expression		*P* value
		Negative	Positive	
Sex	Male	25	7	0.255
	Female	6	4	
Age (Years)	<60	14	4	0.612
	≥60	17	7	
Stage	I/II	20	6	0.559
	III/IV	11	5	

in patient tissue samples. Specimens from 4 subtypes of T cell lymphoma/leukemia were analyzed: peripheral T cell lymphoma, not otherwise specified (PTCL, NOS); angioimmunoblastic T cell lymphoma (AITL); NK/T; and T-LBL/ALL. Lymph nodes (both normal and reactive hyperplastic) and thymus (both normal and hyperplastic) were utilized as controls. IHC staining with an anti-PFKP antibody showed nuclear PFKP enrichment in cells from invasive T cell lymphoma/leukemia (Figure 8A). Statistically, only aggressive T cell lymphoma/leukemia (including PTCL, NOS; AITL; NK/T; and T-LBL/ALL) showed nuclear PFKP staining (Figure 8B), in contrast with specimens from patients with normal T lymph node and reactive hyperplasia, which showed an absence of nuclear PFKP. As a parallel control, the expression of nuclear PFKP in the thymus was comparatively low (Supplemental Figure 8A). Notably, survival rates of both NK/T and AITL lymphoma patients with positive nuclear PFKP staining were significantly decreased compared with those with negative nuclear PFKP staining (Figure 8C). We further performed multivariate prognostic analysis of independent risk factors for OS in patients with AITL, and the result showed that age and nuclear PFKP staining can be utilized as independent prognostic factors (Supplemental Figure 8B). There was no significant correlation between nuclear PFKP expression and sex, age, or stage (Table 4). Consistent with the mechanistic study, the expression of CDK6 was correlated with CXCR4, both of which were highly expressed in NK/T (Supplemental Figure 8, C and D). This was not observed in normal/hyperplastic lymph node controls (Supplemental Figure 8C). Overall, these findings point to the potential utility of nuclear enrichment of PFKP as a novel diagnostic marker for aggressive T cell lymphoma/leukemia.

In summary, these studies demonstrate that PFKP is a nucleocytoplasmic shuttling protein. Nuclear exportation of PFKP depends on its own NESs and the interaction with CRM1, while nuclear importation of PFKP relies on its NLS and the interaction with importin-9. Cyclin D3/CDK6 regulates the nuclear importation of PFKP by exposing a hidden NLS on the protein surface. Nuclear PFKP promotes leukemia cell homing/infiltration by upregulating CXCR4 expression (Figure 8D), and this regulation is c-Myc dependent. Nuclear PFKP enrichment may have prognostic value for T cell lymphoma/leukemia, as it is only observed in aggressive T cell malignancy and correlates negatively with survival rates in patients with T cell malignancies.

Discussion

Metabolic enzymes are important components of cell metabolic reactions that provide energy as well as building materials. Glycolytic enzymes are normally present in the cytoplasm, catalyzing glucose oxidation to generate ATP. Recent studies showed that acetylated PFKP translocates to the plasma membrane to be phosphorylated by EGFR. Phosphorylated PFKP interacts with p85a on the plasma membrane to activate the PI3K pathway (8). Besides those on the plasma membrane, multiple glycolysis component enzymes were also documented in the nucleus to perform novel and significant tumorigenic functions (56). PFKP was found to function in the regulation of gene transcription in breast cancer cells via its interaction with the YAP/TAZ transcriptional cofactors TEADs (10). To date, it was not known how PFKP translocates into the nucleus to perform its function. The results of this study reveal that PFKP is a nucleocytoplasmic shuttling protein. Nuclear import of PFKP relies on its NLS and its interaction with importin-9, while nuclear export of PFKP depends on its NESs' interaction with CRM1. Our experiments revealed that the functional NLS is located at the interface of dimeric PFKP (Figure 1H), which in the tetrameric form is normally shielded. This finding suggests that the dimeric form of PFKP has more nuclear shuttling capability than the tetrameric form. Indeed, we showed the nuclear fraction of dimeric PFKP to be greater than the cytoplasmic fraction. Cyclin D3/CDK6 regulates the interaction between PFKP and importin-9 (Figure 2, E and F), possibly by inducing the formation of dimeric PFKP to expose its functional NLS. Meanwhile, no significant change in the interaction between PFKP and CRM1 was observed in leukemia cells in which CDK6 was inhibited or depleted (Figure 2, E and F), nor did CDK6 depletion affect nuclear accumulation of NLS-PFKP. All these results suggest that CDK6 regulates the nuclear import of PFKP, but not its nuclear export and nuclear retention.

The indispensability of CXCR4 for homing and maintenance of hematopoietic progenitor cells in stromal cell niches within the bone marrow microenvironment has been reported (57, 58). In vivo studies have also shown that CXCR4 induces leukemia cell homing to the marrow (59, 60). Leukemia is frequently widespread and disseminated at diagnosis. It is still critical to understand the mechanisms of leukemia cell trafficking and homing, not only to devise means to prevent further bone marrow homing of the leukemia, but also to provide potential strategies based on mobilizing leukemia cells from the marrow into the peripheral blood where they are more susceptible to other therapies to overcome drug resistance (61, 62). In addition, extramedullary infiltration leads to the development of leukemic tumors in non-marrow sites and plays critical roles in leukemia progression and chemoresistance, as well as extramedullary relapse in ALL patients (63, 64). It is important to elucidate the mechanisms regulating leukemia extramedullary infiltration. Our study revealed a nuclear function of PFKP in promoting T-ALL bone marrow homing and extramedullary infiltration through upregulating CXCR4 expression. The glycolytic function of PFKP is to phosphorylate fructose 6-phosphate to generate fructose 1,6-biphosphate using ATP as a substrate. We found that expression of the dimeric PFKP mutant, S679E, which has less phosphofructokinase activity than WT-PFKP, promoted CXCR4 expression.

This suggests the kinase activity of PFKP may not be required for its nuclear function in regulating CXCR4 expression. In this study, we found that CXCR4 inhibition by antagonists dramatically decreases nuclear PFKP–dependent leukemia homing to the bone marrow, and also decreases infiltration into the spleen and liver. CXCR4 inhibition may mobilize leukemia cells from the marrow to escape into the bloodstream. However, treatment with CXCR4 antagonists did not significantly increase the percentage of circulating leukemia cells in the bloodstream in mice receiving T-ALL cells (Figures 6C and 7G). CXCL12/CXCR4 signaling plays important roles in leukemia cell survival and proliferation (58, 65). It is possible that the survival and/or proliferation of leukemia cells in the bloodstream were/was inhibited by the CXCR4 antagonists, explaining no increase in leukemia cells in the bloodstream.

The biological functions of CXCR4 are mainly dependent on its affinity for CXCL12. CXCR4 antagonists targeting the CXCL12/CXCR4 axis, such as anti-CXCR4 antibodies and low molecular weight compounds, are well developed (66). Our results showed significant reduction of leukemia cells homing to the bone marrow and trafficking to the spleen and liver in mice treated with the CXCR4 antagonist. Of note, the CXCR4 antagonist treatment did not completely inhibit the trafficking and homing of leukemia cells to bone marrow (Figures 6C and 7G). These findings suggest that blocking the CXCL12/CXCR4 axis may not be sufficient to completely inhibit the homing and infiltration. A recent study showed that CXCR4 has CXCL12-independent roles in protecting acute myeloid leukemia from differentiation (67). CXCL12-independent function(s) of CXCR4 may also contribute to the leukemia homing and infiltration. PFKP has been shown to interact with several transcription factors, which suggests PFKP may have multiple nuclear functions through interacting with various transcription factors to regulate CXCR4-independent leukemia homing/progression (Supplemental Figure 4G). T-ALL bone marrow homing and extramedullary infiltration were decreased/inhibited if nuclear translocation of PFKP was prevented, as shown in leukemia cells expressing PFKP-RXL (Figure 6C). The significance of nuclear PFKP in promoting leukemia bone marrow homing and extramedullary infiltration was also reflected in patient-derived primary T-ALL cells (Figure 7G). These findings suggest that targeting nuclear PFKP or preventing PFKP nuclear translocation has clinical benefit in curtailing leukemia bone marrow homing and extramedullary infiltration. Our study demonstrates the mechanisms underlying PFKP shuttling to the nucleus; further studies are warranted that address means to efficiently block nuclear translocation of PFKP for therapeutic purposes.

CDK6 has functions in leukemia cell proliferation and survival (9). In this study, we found that CDK6 facilitates PFKP nuclear translocation to promote leukemia invasion and homing, indicating that targeting CDK6 may hold promise for treating patients with T cell malignancies. The proteolysis-targeting chimera–based (PROTAC-based) CDK6 degrader BSJ-03-123 efficiently degraded CDK6 to downregulate CXCR4 expression (Figure 4B). Future translational work using preclinical T cell leukemia mouse models may be carried out to establish the therapeutic efficacy of this CDK6 degrader. Alternatively, this study shows that glycolysis inhibition by 2-DG reduces PFKP nuclear accumulation and CXCR4 expression (Supplemental Figure 6, F and G), which suggests that glycolysis modulation may function as a regulatory mechanism in mediating PFKP nuclear translocation, CXCR4 expression, and leukemia bone marrow homing and extramedullary infiltration. Thus, glycolysis inhibition also shows promise as a novel therapeutic method for patients with T cell leukemia.

Novel prognostic markers and efficient therapeutic strategies are still needed for T cell lymphoma/leukemia (68). Expression levels of CXCR4 have been reported to have prognostic value in certain categories of T cell lymphoma/leukemia (69–71). The current study demonstrates that nuclear PFKP is involved in T cell leukemia homing and infiltration via upregulating CXCR4. We showed that primary human T-ALL cells with high nuclear PFKP levels displayed enhanced expression levels of CXCR4 and cell invasion/homing capabilities. In addition, the analysis of clinical tissue specimens showed that nuclear PFKP was expressed in T lymphocytes from invasive T cell lymphoma/leukemia patients, but not in cells of nonmalignant lymph node/thymus (Figure 8, A and B, and Supplemental Figure 8A). The presence of nuclear PFKP in T cell lymphoma patients correlated well with the OS (Figure 8C). Altogether, these results point to the potential application of nuclear PFKP as a novel prognostic marker for T cell lymphoma/leukemia.

Methods

Further details of the methods are provided in the supplemental material.

Patient-derived primary cells. Primary human leukemia cells derived from deidentified T-ALL patients (CBAT-93917, DFAT-24836, and DFAT-28537) were purchased from PROXE (Public Repository of Xenografts, Dana-Farber Cancer Institute [DFCI]) through the DFCI Center for Patient Derived Models. These leukemia cells were expanded as primary xenografts (patient-derived xenografts [PDXs]) in immunodeficient NSG mice at very low passages, which are the most useful source of primary cells (55). In vitro primary human T-ALL samples were cultured in α-minimum essential media with 1× GlutaMAX (GIBCO, 32571-036) containing 10% FBS, 10% human AB serum (MilliporeSigma, H4522), 1% L-glutamine, 1% penicillin/streptomycin, 1× Insulin-Transferrin-Selenium (GIBCO, 41100-045), 10 ng/mL recombinant mouse IL-7 (Peprotech, 217-17), and 10 ng/mL recombinant human IL-2 (Peprotech, 200-02).

In vivo experiments. For survival analysis, 8-week-old female immunodeficient NOD.Cg-Prkdc<scid>IL2rg<tm1Sug>/JicTac (NOG) mice purchased from Taconic were transplanted i.v. with KOPTK1 cells (2×10^6) expressing WT-PFKP, NLS-PFKP, or PFKP-RXL ($n = 10$ per group). Each group of mice was unbiasedly subdivided into 2 subgroups ($n = 5$/subgroup). Seven days after cell injection, one subgroup received the CXCR4 antagonist (plerixafor, 5 mg/kg) treatment 6 days a week via i.p. injection, and the other group received drug vehicle (PBS) as a control.

For leukemia homing/infiltration analysis, immunodeficient mice were randomly assigned to 3 experimental groups receiving 2×10^6 KOPTK1 cells expressing WT-PFKP ($n = 12$), NLS-PFKP ($n = 12$), or PFKP-RXL ($n = 10$) via tail vein injection. Each group of mice was unbiasedly subdivided into 2 subgroups ($n = 6$ for WT- and NLS-PFKP, $n = 5$ for PFKP-RXL per subgroup): one subgroup received plerixafor (5 mg/kg) treatment 6 days a week via i.p. injection started on the same day as leukemia cell injection, and the other subgroup received drug vehicle (PBS) as a control. Tumor-bearing mice were sacrificed on

day 24. For experiments with primary T-ALL, DFAT-24836 or DFAT-28537 cells (1×10^6) were tail vein injected in immunodeficient NSG mice (n = 10/group). Each group of mice was unbiasedly subdivided into 2 subgroups (n = 5/subgroup). One subgroup received plerixafor (5 mg/kg) treatment 6 days a week started on the same day as primary T-ALL cell injection, and the other subgroup received PBS as a control. Tumor-bearing mice were sacrificed on day 29. Mouse peripheral blood/bone marrow (from femurs)/spleen/liver was collected to analyze the presence of leukemia (flow cytometry analysis gated on human $CD45^+$ cells). Red blood cells were lysed using 1× lysis buffer (BD Biosciences, 555899). The remaining cells were stained with anti–human CD45 antibody (BioLegend, 304032). For tumor-bearing mice implanted with KOPTK1 cells, a portion of the collected tissues (spleen, liver, femurs) from individual mice was fixed in formaldehyde for 24 hours, and femurs were decalcified in 9% formic acid for an additional 2 days followed by paraffin embedding. Anti–human CD45 antibody (1:100 dilution) was applied to detect human leukemia cells for IHC staining. No animals were excluded from the analysis. The investigators were not blinded to group allocation.

Cell invasion assay. Each Transwell of a 24-well Transwell-inserted plate (Boyden chamber) was coated with 50 μL Matrigel (Thermo Fisher Scientific, CB-40234) diluted 1:2 or 1:4 in RPMI 1640 medium supplemented with 2% FBS at 37°C for 30 minutes. Cells (5×10^5 to 10×10^5) suspended in 100 μL RPMI 1640 with 2% FBS without human CXCL12 were seeded onto the upper chambers of the 24-well Transwell-inserted plate (5 μm polycarbonate membrane, Corning, CLS3421). RPMI 1640 medium (600 μL) supplemented with 2% FBS and 100 ng/mL human CXCL12 was added to the bottom chamber of the Transwell plates. RPMI 1640 medium supplemented with 2% FBS without human CXCL12 added to the bottom chamber was used as a control. The invasion assay ran for 8 to 24 hours, at which point the invading cells in the bottom chamber were collected and counted.

Statistics. Group comparisons were performed using 2-sample t tests. A P value of less than 0.05 was considered statistically significant, and P greater than 0.05 not significant (NS). Multivariate Cox regression analysis was performed to search for independent risk factors (including age, sex, stage, and nuclear PFKP staining) for OS in patients with AITL using the "survival" package in version 4.0.3 of R software (https://www.r-project.org/). Correlations between nuclear PFKP expression levels and clinicopathological features in patients with AITL were calculated and evaluated by the χ^2 test with SPSS software (IBM) ($n > 40$).

Study approval. All mouse experiments were carried out according to protocols approved by the Institutional Animal Care and Use Committee of the Medical University of South Carolina. The human specimens used in this study were approved by the Ethics Committee of Tongji Medical College, Huazhong University of Science and Technology, and signed informed consent was obtained from all patients' families.

Author contributions

XG and HW conceived and designed experiments. XG, SQ, and HW performed the experiments. SQ, DK, and XW performed the patient sample study. YW helped with the mouse experiments. CC performed bioinformatics analysis. BJ helped with drug preparation. JZ provided reagents. RJH, AM, KDT, GWL, and XZY provided advisory support. XG and HW wrote manuscript with all authors' input. HW supervised the project.

Acknowledgments

We thank Peter Sicinski (Dana-Farber Cancer Institute, Harvard Medical School) for sharing reagents, including cell lines and plasmids, for this project. This research was supported by the National Natural Science Foundation of China (grant 81700012 to SQ); the NIH (R01 HL140953 to XZY); a National Institute of General Medical Sciences, National Institutes of Health Institutional Developmental Award (COBRE) (5P20GM103542-08 to HW); Swim Across America (A20-0218-001 to HW); American Cancer Society Institutional Research Award (ACS-IRG) (IRG-19-137-20 to HW); and a Bristol-Myers Squibb – Melanoma Research Alliance (MRA) Young Investigator Award (821901 to HW); and the NIH (R37CA251165 to HW).

Address correspondence to: Haizhen Wang, Department of Cell and Molecular Pharmacology & Experimental Therapeutics, Medical University of South Carolina, Charleston, South Carolina 29425, USA. Phone: 843.792.2669; Email: wangha@musc.edu.

1. Cairns RA, et al. Regulation of cancer cell metabolism. *Nat Rev Cancer*. 2011;11(2):85–95.
2. Yi W, et al. Phosphofructokinase 1 glycosylation regulates cell growth and metabolism. *Science*. 2012;337(6097):975–980.
3. Vora S, et al. Alterations in the activity and isozymic profile of human phosphofructokinase during malignant transformation in vivo and in vitro: transformation- and progression-linked discriminants of malignancy. *Cancer Res*. 1985;45(7):2993–3001.
4. Sanchez-Martinez C, Aragon JJ. Analysis of phosphofructokinase subunits and isozymes in ascites tumor cells and its original tissue, murine mammary gland. *FEBS Lett*. 1997;409(1):86–90.
5. Moon JS, et al. Krüppel-like factor 4 (KLF4) activates the transcription of the gene for the platelet isoform of phosphofructokinase (PFKP) in breast cancer. *J Biol Chem*. 2011;286(27):23808–23816.
6. Lee JH, et al. Stabilization of phosphofructokinase 1 platelet isoform by AKT promotes tumorigenesis. *Nat Commun*. 2017;8(1):949.
7. Luo X, et al. The platelet isoform of phosphofructokinase in acute myeloid leukemia: clinical relevance and prognostic implication. *Blood*. 2018;132(Supplement 1):5251.
8. Lee JH, et al. EGFR-phosphorylated platelet isoform of phosphofructokinase 1 promotes PI3K activation. *Mol Cell*. 2018;70(2):197–210.
9. Wang H, et al. The metabolic function of cyclin D3-CDK6 kinase in cancer cell survival. *Nature*. 2017;546(7658):426–430.
10. Enzo E, et al. Aerobic glycolysis tunes YAP/TAZ transcriptional activity. *EMBO J*. 2015;34(10):1349–1370.
11. Malumbres M. Cyclin-dependent kinases. *Genome Biol*. 2014;15(6):122.
12. Yu Q, et al. Requirement for CDK4 kinase function in breast cancer. *Cancer Cell*. 2006;9(1):23–32.
13. Choi YJ, et al. The requirement for cyclin D function in tumor maintenance. *Cancer Cell*. 2012;22(4):438–451.
14. Sherr CJ, et al. Targeting CDK4 and CDK6: from discovery to therapy. *Cancer Discov*. 2016;6(4):353–367.
15. Anders L, et al. A systematic screen for CDK4/6 substrates links FOXM1 phosphorylation to senescence suppression in cancer cells. *Cancer Cell*. 2011;20(5):620–634.
16. Matsuura I, et al. Cyclin-dependent kinases regulate the antiproliferative function of Smads. *Nature*. 2004;430(6996):226–231.
17. Hu MG, et al. CDK6 kinase activity is required for thymocyte development. *Blood*. 2011;117(23):6120–6131.
18. Zhang J, et al. Cyclin D-CDK4 kinase destabilizes PD-L1 via cullin 3-SPOP to control cancer immune surveillance. *Nature*. 2018;553(7686):91–95.
19. Lien HC, Lin CW, Huang PH, Chang ML, Hsu SM. Expression of cyclin-dependent kinase 6 (cdk6) and frequent loss of CD44 in nasal-nasopharyngeal NK/T-cell lymphomas: comparison

with CD56-negative peripheral T-cell lymphomas. *Lab Invest*. 2000;80(6):893–900.
20. Sawai CM, et al. Therapeutic targeting of the cyclin D3:CDK4/6 complex in T cell leukemia. *Cancer Cell*. 2012;22(4):452–465.
21. Girardi T, et al. The genetics and molecular biology of T-ALL. *Blood*. 2017;129(9):1113–1123.
22. Hu MG, et al. A requirement for cyclin-dependent kinase 6 in thymocyte development and tumorigenesis. *Cancer Res*. 2009;69(3):810–818.
23. Shin SS, et al. MicroRNA-892b influences proliferation, migration and invasion of bladder cancer cells by mediating the p19ARF/cyclin D1/CDK6 and Sp-1/MMP-9 pathways. *Oncol Rep*. 2016;36(4):2313–2320.
24. Geng B, et al. An TRIM59-CDK6 axis regulates growth and metastasis of lung cancer. *J Cell Mol Med*. 2019;23(2):1458–1469.
25. Gao X, et al. Cyclin D-CDK4/6 functions in cancer. *Adv Cancer Res*. 2020;148:147–169.
26. Balkwill F. Cancer and the chemokine network. *Nat Rev Cancer*. 2004;4(7):540–550.
27. Mortezaee K. CXCL12/CXCR4 axis in the microenvironment of solid tumors: a critical mediator of metastasis. *Life Sci*. 2020;249:117534.
28. Zagzag D, et al. Stromal cell-derived factor-1alpha and CXCR4 expression in hemangioblastoma and clear cell-renal cell carcinoma: von Hippel-Lindau loss-of-function induces expression of a ligand and its receptor. *Cancer Res*. 2005;65(14):6178–6188.
29. Salcedo R, et al. Vascular endothelial growth factor and basic fibroblast growth factor induce expression of CXCR4 on human endothelial cells: in vivo neovascularization induced by stromal-derived factor-1alpha. *Am J Pathol*. 1999;154(4):1125–1135.
30. Phillips RJ, et al. Epidermal growth factor and hypoxia-induced expression of CXC chemokine receptor 4 on non-small cell lung cancer cells is regulated by the phosphatidylinositol 3-kinase/PTEN/AKT/mammalian target of rapamycin signaling pathway and activation of hypoxia inducible factor-1alpha. *J Biol Chem*. 2005;280(23):22473–22481.
31. Zheng J. Energy metabolism of cancer: glycolysis versus oxidative phosphorylation (Review). *Oncol Lett*. 2012;4(6):1151–1157.
32. Pemberton LF, Paschal BM. Mechanisms of receptor-mediated nuclear import and nuclear export. *Traffic*. 2005;6(3):187–198.
33. Fornerod M, et al. CRM1 is an export receptor for leucine-rich nuclear export signals. *Cell*. 1997;90(6):1051–1060.
34. Lange A, et al. Classical nuclear localization signals: definition, function, and interaction with importin alpha. *J Biol Chem*. 2007;282(8):5101–5105.
35. Xu D, et al. Sequence and structural analyses of nuclear export signals in the NESdb database. *Mol Biol Cell*. 2012;23(18):3677–3693.
36. Wang H, et al. P68 RNA helicase is a nucleocytoplasmic shuttling protein. *Cell Res*. 2009;19(12):1388–1400.
37. Kloos M, et al. Crystal structure of human platelet phosphofructokinase-1 locked in an activated conformation. *Biochem J*. 2015;469(3):421–432.
38. Ma T, et al. Interaction between cyclin-dependent kinases and human papillomavirus replication-initiation protein E1 is required for efficient viral replication. *Proc Natl Acad Sci U S A*. 1999;96(2):382–387.
39. Topacio BR, et al. Cyclin D-Cdk4,6 drives cell-cycle progression via the retinoblastoma protein's C-terminal helix. *Mol Cell*. 2019;74(4):758–770.
40. Chook YM, Suel KE. Nuclear import by karyopherin-βs: recognition and inhibition. *Biochim Biophys Acta*. 2011;1813(9):1593–1606.
41. Mehta SA, et al. Negative regulation of chemokine receptor CXCR4 by tumor suppressor p53 in breast cancer cells: implications of p53 mutation or isoform expression on breast cancer cell invasion. *Oncogene*. 2007;26(23):3329–3337.
42. Powell E, et al. Contribution of p53 to metastasis. *Cancer Discov*. 2014;4(4):405–414.
43. Dang CV. MYC on the path to cancer. *Cell*. 2012;149(1):22–35.
44. Liu H, et al. Redeployment of Myc and E2f1-3 drives Rb-deficient cell cycles. *Nat Cell Biol*. 2015;17(8):1036–1048.
45. Delmore JE, et al. BET bromodomain inhibition as a therapeutic strategy to target c-Myc. *Cell*. 2011;146(6):904–917.
46. Gomez-Curet I, et al. c-Myc inhibition negatively impacts lymphoma growth. *J Pediatr Surg*. 2006;41(1):207–211.
47. Huang MJ, et al. A small-molecule c-Myc inhibitor, 10058-F4, induces cell-cycle arrest, apoptosis, and myeloid differentiation of human acute myeloid leukemia. *Exp Hematol*. 2006;34(11):1480–1489.
48. Chang CY, et al. The metabolic regulator ERRα, a downstream target of HER2/IGF-1R, as a therapeutic target in breast cancer. *Cancer Cell*. 2011;20(4):500–510.
49. O'Callaghan K, et al. Targeting CXCR4 with cell-penetrating pepducins in lymphoma and lymphocytic leukemia. *Blood*. 2012;119(7):1717–1725.
50. Teicher BA, Fricker SP. CXCL12 (SDF-1)/CXCR4 pathway in cancer. *Clin Cancer Res*. 2010;16(11):2927–2931.
51. Kufareva I, et al. Stoichiometry and geometry of the CXC chemokine receptor 4 complex with CXC ligand 12: molecular modeling and experimental validation. *Proc Natl Acad Sci U S A*. 2014;111(50):E5363–E5372.
52. Uy GL, et al. Plerixafor, a CXCR4 antagonist for the mobilization of hematopoietic stem cells. *Expert Opin Biol Ther*. 2008;8(11):1797–1804.
53. Peled A, et al. The high-affinity CXCR4 antagonist BKT140 is safe and induces a robust mobilization of human $CD34^+$ cells in patients with multiple myeloma. *Clin Cancer Res*. 2014;20(2):469–479.
54. Curtis M, et al. Fibroblasts mobilize tumor cell glycogen to promote proliferation and metastasis. *Cell Metab*. 2019;29(1):141–155.
55. Morita K, et al. Allosteric activators of protein phosphatase 2A display broad antitumor activity mediated by dephosphorylation of MYBL2. *Cell*. 2020;181(3):702–715.
56. Lu Z, Hunter T. Metabolic kinases moonlighting as protein kinases. *Trends Biochem Sci*. 2018;43(4):301–310.
57. Broxmeyer HE, et al. Rapid mobilization of murine and human hematopoietic stem and progenitor cells with AMD3100, a CXCR4 antagonist. *J Exp Med*. 2005;201(8):1307–1318.
58. Burger JA, Burkle A. The CXCR4 chemokine receptor in acute and chronic leukaemia: a marrow homing receptor and potential therapeutic target. *Br J Haematol*. 2007;137(4):288–296.
59. Sipkins DA, et al. In vivo imaging of specialized bone marrow endothelial microdomains for tumour engraftment. *Nature*. 2005;435(7044):969–973.
60. Burger JA, Peled A. CXCR4 antagonists: targeting the microenvironment in leukemia and other cancers. *Leukemia*. 2009;23(1):43–52.
61. Jung MJ, et al. Upregulation of CXCR4 is functionally crucial for maintenance of stemness in drug-resistant non-small cell lung cancer cells. *Oncogene*. 2013;32(2):209–221.
62. Xie S, et al. CXCR4 promotes cisplatin-resistance of non-small cell lung cancer in a CYP1B1-dependent manner. *Oncol Rep*. 2017;37(2):921–928.
63. Gunes G, et al. Extramedullary relapses of acute leukemias after allogeneic hematopoietic stem cell transplantation: clinical features, cumulative incidence, and risk factors. *Bone Marrow Transplant*. 2019;54(4):595–600.
64. Yu J, et al. Incidence, risk factors and outcome of extramedullary relapse after allogeneic hematopoietic stem cell transplantation in patients with adult acute lymphoblastic leukemia. *Ann Hematol*. 2020;99(11):2639–2648.
65. Cancilla D, et al. Targeting CXCR4 in AML and ALL. *Front Oncol*. 2020;10:1672.
66. Chatterjee S, et al. The intricate role of CXCR4 in cancer. *Adv Cancer Res*. 2014;124:31–82.
67. Ramakrishnan R, et al. CXCR4 signaling has a CXCL12-independent essential role in murine MLL-AF9-driven acute myeloid leukemia. *Cell Rep*. 2020;31(8):107684.
68. Piccaluga PP, et al. Prognostic markers in peripheral T-cell lymphoma. *Curr Hematol Malig Rep*. 2010;5(4):222–228.
69. Weng AP, et al. CXCR4/CD184 immunoreactivity in T-cell non-Hodgkin lymphomas with an overall $Th1^-$ $Th2^+$ immunophenotype. *Am J Clin Pathol*. 2003;119(3):424–430.
70. Yu ZZ, et al. [Significance of CXCL12/CXCR4 expression in T-lymphoblastic lymphoma/leukemia]. *Zhonghua Bing Li Xue Za Zhi*. 2016;45(12):838–843.
71. Yang K, et al. Expression and significance of CD47, PD1 and PDL1 in T-cell acute lymphoblastic lymphoma/leukemia. *Pathol Res Pract*. 2019;215(2):265–271.